

MARTIN MARETTA ENERGY SYSTEMS LIBRARIES



3 4456 0321298 5

NUREG/CR-5712  
(ORNL/TM-11823)

---

# MORECA: A Computer Code for Simulating Modular High-Temperature Gas-Cooled Reactor Core Heatup Accidents

---

Prepared by  
S. J. Ball

**Oak Ridge National Laboratory**

Prepared for  
**U.S. Nuclear Regulatory Commission**

OAK RIDGE NATIONAL LABORATORY

CENTRAL RESEARCH LIBRARY

CIRCULATION SECTION

4500N ROOM 175

**LIBRARY LOAN COPY**

DO NOT TRANSFER TO ANOTHER PERSON

If you wish someone else to see this  
report, send in name with report and  
the library will arrange a loan.

UCN 59813 572

## AVAILABILITY NOTICE

### Availability of Reference Materials Cited in NRC Publications

Most documents cited in NRC publications will be available from one of the following sources:

1. The NRC Public Document Room, 2120 L Street, NW, Lower Level, Washington, DC 20555
2. The Superintendent of Documents, U.S. Government Printing Office, P.O. Box 37082, Washington, DC 20513-7082
3. The National Technical Information Service, Springfield, VA 22161

Although the listing that follows represents the majority of documents cited in NRC publications, it is not intended to be exhaustive.

Referenced documents available for inspection and copying for a fee from the NRC Public Document Room include NRC correspondence and internal NRC memoranda; NRC Office of Inspection and Enforcement bulletins, circulars, information notices, inspection and investigation notices; Licensee Event Reports; vendor reports and correspondence; Commission papers; and applicant and licensee documents and correspondence.

The following documents in the NUREG series are available for purchase from the GPO Sales Program: formal NRC staff and contractor reports, NRC-sponsored conference proceedings, and NRC booklets and brochures. Also available are Regulatory Guides, NRC regulations in the *Code of Federal Regulations*, and *Nuclear Regulatory Commission Issuances*.

Documents available from the National Technical Information Service include NUREG series reports and technical reports prepared by other federal agencies and reports prepared by the Atomic Energy Commission, forerunner agency to the Nuclear Regulatory Commission.

Documents available from public and special technical libraries include all open literature items, such as books, journal and periodical articles, and transactions. Federal Register notices, federal and state legislation, and congressional reports can usually be obtained from these libraries.

Documents such as theses, dissertations, foreign reports and translations, and non-NRC conference proceedings are available for purchase from the organization sponsoring the publication cited.

Single copies of NRC draft reports are available free, to the extent of supply, upon written request to the Office of Information Resources Management, Distribution Section, U.S. Nuclear Regulatory Commission, Washington, DC 20555.

Copies of industry codes and standards used in a substantive manner in the NRC regulatory process are maintained at the NRC Library, 7920 Norfolk Avenue, Bethesda, Maryland, and are available there for reference use by the public. Codes and standards are usually copyrighted and may be purchased from the originating organization or, if they are American National Standards, from the American National Standards Institute, 1430 Broadway, New York, NY 10018.

## DISCLAIMER NOTICE

This report was prepared as an account of work sponsored by an agency of the United States Government. Neither the United States Government nor any agency thereof, or any of their employees, makes any warranty, expressed or implied, or assumes any legal liability or responsibility for any third party's use, or the results of such use, of any information, apparatus, product or process disclosed in this report, or represents that its use by such third party would not infringe privately owned rights.

NUREG/CR-5712  
ORNL/TM-11823  
R1, R7, R8

---

---

# MORECA: A Computer Code for Simulating Modular High-Temperature Gas-Cooled Reactor Core Heatup Accidents

---

---

Manuscript Completed: April 1991  
Date Published: October 1991

Prepared by  
S. J. Ball

Oak Ridge National Laboratory  
Operated by Martin Marietta Energy Systems, Inc.

Oak Ridge National Laboratory  
Oak Ridge, TN 37831-6285

Prepared for  
Division of Regulatory Applications  
Office of Nuclear Regulatory Research  
U.S. Nuclear Regulatory Commission  
Washington, DC 20555  
NRC FIN A9477  
Under Contract No. DE-AC05-84OR21400



3 4456 0321298 5



## ABSTRACT

The design features of the modular high-temperature gas-cooled reactor (MHTGR) have the potential to make it essentially invulnerable to damage from postulated core heatup accidents. This report describes the ORNL MORECA code, which was developed for analyzing postulated long-term core heatup scenarios for which active cooling systems used to remove afterheat following the accidents can be assumed to be unavailable. Simulations of long-term loss-of-forced-convection accidents, both with and without depressurization of the primary coolant, have shown that maximum core temperatures stay below the point at which any significant fuel failures and fission product releases are expected. Sensitivity studies also have been done to determine the effects of errors in the predictions due both to uncertainties in the modeling and to the assumptions about operational parameters. MORECA models the U. S. Department of Energy reference design of a standard MHTGR. This program was sponsored by the U.S. Nuclear Regulatory Commission to assist in the preliminary determinations of licensability of the reactor design.



## CONTENTS

	<u>Page</u>
ABSTRACT .....	iii
LIST OF FIGURES .....	vii
1. INTRODUCTION .....	1
2. MHTGR DESCRIPTION .....	2
3. MORECA CODE SUMMARY DESCRIPTION .....	4
3.1 CORE MODEL .....	4
3.2 CORE BYPASS FLOW MODELING .....	5
3.3 PLENUM MODELS .....	6
3.4 CORE BARREL AND VESSEL MODELS .....	6
3.5 REACTOR CAVITY COOLING SYSTEM MODEL .....	7
3.6 SHUTDOWN COOLING SYSTEM MODEL .....	7
3.7 FUEL FAILURE MODELS .....	8
4. SUMMARY OF MORECA RUNS, CAPABILITIES, AND FINDINGS .....	9
4.1 ACCIDENT SCENARIO SENSITIVITY STUDIES .....	9
4.2 COMPLETE RCCS FAILURE .....	12
4.3 INTERACTIVE WORKSTATION VERSION OF MORECA .....	13
4.4 CONCLUSIONS .....	13
5. REFERENCES .....	15
Appendix A. DETAILED MODEL DESCRIPTIONS .....	17
Appendix B. MORECA INPUT VARIABLES .....	39
Appendix C. MORECA PROGRAM DESCRIPTION DATABASES .....	45



## LIST OF FIGURES

Figure	Page
1. The 350-MW(t) modular high-temperature gas-cooled reactor module . . . . .	3
2. Reference case depressurized loss of forced convection accident with reactor cavity cooling system operational, temperatures of core and vessel vs time . . . . .	10
3. Reference case pressurized loss of forced convection accident with reactor cavity cooling system operational, temperatures of core and vessel vs time . . . . .	10
4. Reference case depressurized loss of forced convection accident with reactor cavity cooling system not operational, temperatures of core and vessel vs time . . . . .	14
5. MORECA Interactive workstation version accident scenario display screen . . . .	14
A.1. Standard fuel element. . . . .	20
A.2. Comparison of coolant heat transfer methods . . . . .	26
A.3. Ring-to-disk view factors . . . . .	28
A.4. Passive reactor cavity cooling system . . . . .	32
C.1. OREP program . . . . .	48
C.2. MORECA input variables . . . . .	49
C.3. Listing of variables in common block PASS . . . . .	49
C.4. ORECOM file of variables in common blocks and subroutines in which they appear . . . . .	50
C.5. Listing of variables defined and modified in subroutine BOTTEM . . . . .	51
C.6. PROCAL listing . . . . .	53
C.7. PPCAL program . . . . .	60
C.8. DIDMOD program . . . . .	61



## 1. INTRODUCTION

The MORECA code was developed under sponsorship of the U.S. Nuclear Regulatory Commission, Office of Nuclear Regulatory Research (NRC-RES). The objective of the task was to perform independent analyses of a broad range of long-term core heatup accident scenarios for the modular high-temperature gas-cooled reactor (MHTGR). The reference design analyzed was the standard commercial plant version sponsored by the U.S. Department of Energy, Office of Nuclear Energy (DOE-NE).

MORECA is based on the Oak Ridge National Laboratory (ORNL) ORECA code, which was also developed under NRC sponsorship and which has been in use at ORNL and elsewhere since 1975 (Ref. 1). ORECA has been used in accident studies requiring core thermal analysis of the Fort St. Vrain (FSV) reactor (Refs. 2 and 3), the DOE 2240-MW(t) design (Ref. 4), and several other HTGR designs. ORECA-FSV has been partially verified and validated for numerous cases vs FSV data (Ref. 5) and General Atomics (GA) proprietary codes. Verification of MORECA and other versions of ORECA has been limited to comparisons with GA and Brookhaven National Laboratory (BNL) code calculations. These activities are continuing in order to verify model applicability to wider classes of transients and accidents.

MORECA is a fast-running code, thereby permitting reasonably efficient accident scenario and parameter sensitivity investigations. There are currently five versions of MORECA. Simulations of both the commercial and the DOE New Production Reactor (NPR) MHTGRs each have a batch-input serial version (using standard Fortran-77) and a parallel version (using Encore parallel Fortran). The batch-input serial codes have been run and tested on many different platforms (VAX, IBM, PC, CRAY, and Encore) and are therefore readily portable to most installations. The parallel versions interface the ORNL Encore Multimax 320 Parallel Processor with a SUN workstation to permit on-line user interactions, and they can run accident transients at up to 1000 times faster than real time (Ref. 6). These versions are portable only to installations having an Encore and SUN workstation network. Recently, the commercial plant serial version was adapted to the SUN interface program and can now run "stand-alone" on a SUN workstation. Using the SUN SPARCstation-2 workstation, accident transients can now be run with an interactive display at up to 1400 times faster than real time. The commercial versions are supported by NRC-RES and the NPRs by DOE-NP. Analyses using the commercial MHTGR versions were done in support of the NRC Safety Evaluation Report (Ref. 7).

## 2. MHTGR DESCRIPTION

The design features of the DOE-NE Standard Commercial MHTGR are shown in Fig. 1. Each of four reactor modules consists of a tall cylindrical ceramic core with a thermal power rating of 350 MW, and a single once-through steam generator with a superheater to provide high-temperature [538°C, (1000°F)] steam to a steam header and turbine plant common to two or more modules. Design trade studies are currently considering other balance-of-plant (BOP) arrangements and higher rated power levels. The rated output of the four-module plant is 540 MW(e), with a net thermal efficiency of 39%. The high-pressure [6.38 MPa (925 psia)] helium coolant is driven downward through the core by a single motor-driven circulator. A smaller capacity circulator-heat exchanger loop, the shutdown cooling system (SCS), is located within the reactor vessel and is used for decay heat removal during maintenance. In cases for which neither the main nor the SCS loop is available, afterheat is removed by the passive, safety-grade air-cooled reactor cavity cooling system (RCCS), which is in operation at all times and which does not require any operator or automatic actuation. There is no conventional containment building, because the multilayered porous and dense carbon and silicon carbide coatings on the microscopic fuel particles are proposed by DOE to be a sufficient fission product barrier.

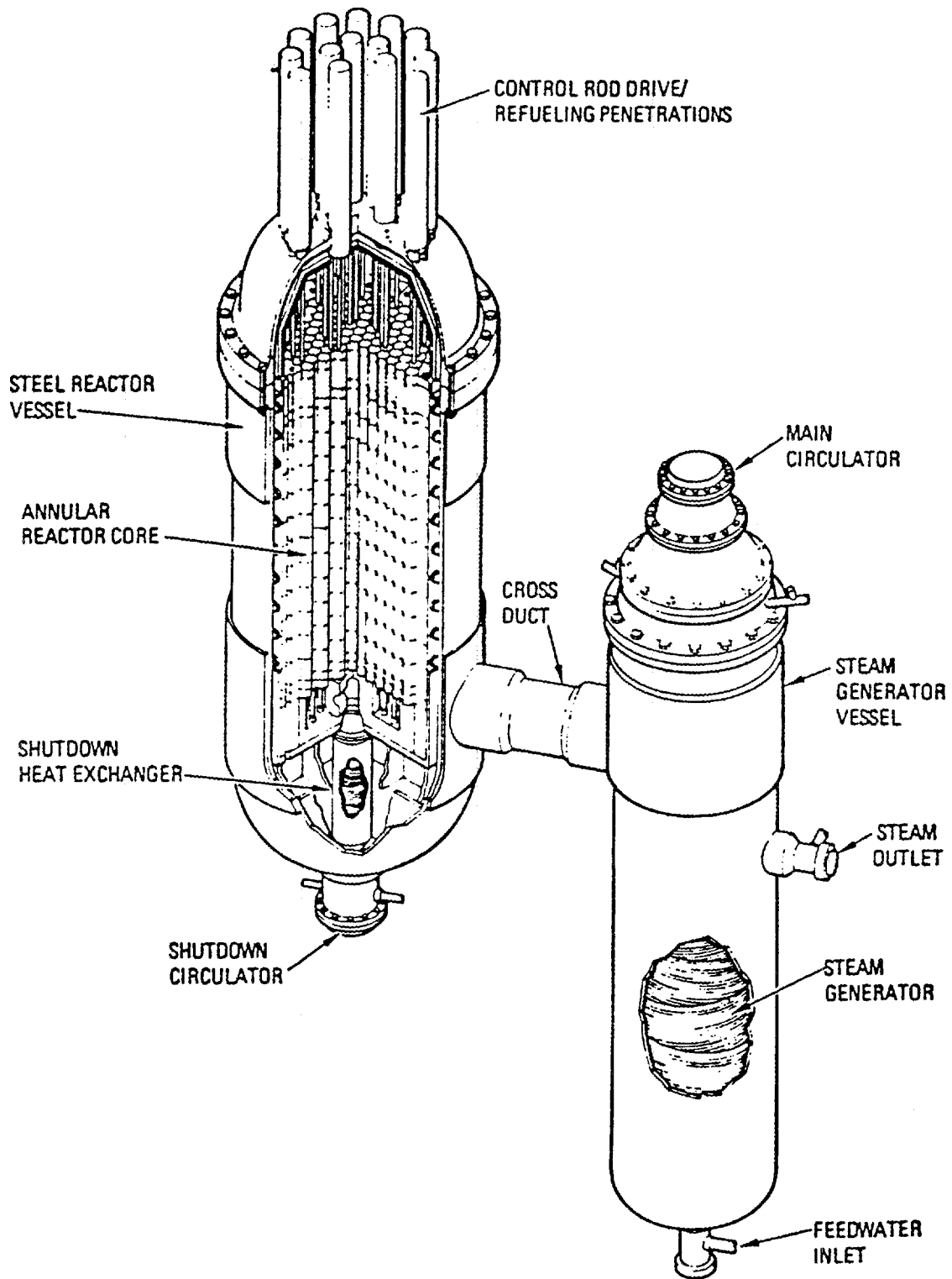


Fig. 1. The 350-MW(t) modular high-temperature gas-cooled reactor module. Source: U.S. Department of Energy, *Licensing Plan for the Standard MHTGR*, HTGR-85-001, Rev. 3, 1986 (this document is classified as "Applied Technology" and is not in the public domain; requests for this document should be made through the U.S. Department of Energy, Washington, D.C.).

### 3. MORECA CODE SUMMARY DESCRIPTION

Brief descriptions of the models used in the MORECA code are given here. More detailed descriptions of the models, with derivations and equations, are in Appendix A. Input data descriptions and explanations are in Appendix B, and a database identifying all program variables, common blocks, arguments, and subroutines is described in Appendix C. The database has been found to be particularly useful for program verification and modification tasks.

#### 3.1 CORE MODEL

The MORECA code model for the core uses a point heat capacity node for each of the 66 fuel and 139 reflector elements (vs one node per 7-element region in ORECA) in each of the 14 axial regions. The core is thus represented by  $(205 \times 14 =)$  2870 nodes. This finer structure was thought to be appropriate because of the high sensitivity of low fuel failure rates to time-at-temperature transients in the range near 1600°C and because it allows for investigations of azimuthal temperature asymmetries for both core and vessel, a feature that other current MHTGR core codes do not yet have. Radial power peaking factors are utilized on a per-element basis.

Variable core thermal properties as supplied by GA (Ref. 8) were used for reference case calculations. These properties are functions of both temperature and radiation damage. Fully irradiated thermal properties are used for the fuel, the inner reflector, and the ring of outer reflector elements adjacent to the fuel. Currently, the MORECA model does not include effects of annealing, which increases the thermal conductivity of the fuel and adjacent reflectors as the core heats up during the hypothetical accidents. Thermal conductivities for the core materials differ in the radial and axial directions because of graphite's anisotropic properties.

The Preliminary Safety Information Document (PSID, Ref. 9) function for decay heat is used for reference case calculations; it is considerably more conservative than the current "best estimate" function (Ref. 8). The PSID, best estimate, and FSV Final Safety Analysis Report (FSAR) decay heat functions are all available in the code for use in sensitivity studies.

Coolant flow in the core is modeled over the full ranges expected in both normal operation and accidents, including pressurized and depressurized (and in between), for forced and natural circulation, upflow and downflow, and for turbulent, laminar, and transition flow regimes. One-dimensional flow in each of the fuel elements is modeled explicitly.

Coolant flow in the inner and outer reflectors is assumed to be uniformly distributed in the spaces between blocks, where the initial reflector flows start out as user-input fractions of the total forced-circulation flow. Subsequent bypass flows are calculated assuming that the effective gap sizes are fixed. Determination of the actual (nonuniform) flow between blocks would depend on the gap size distributions, which are random and quite variable, and change both with operating conditions and operating history. Sensitivity studies have shown that the at-power core temperature distributions are affected significantly by bypass flow assumptions; however, the peak fuel temperatures in

the core heatup accidents are not. Changes in direction of the inner reflector and outer reflector flows are also accommodated in the model.

The manner in which the flow redistributes itself among the fuel elements is calculated in subroutine CFLOW. The heat transfer between the core and the helium coolant is calculated in subroutine CONVEC. Temperature-variant helium properties are accounted for.

The pressure in the primary loop is calculated by using the perfect gas law, assuming a constant loop inventory and approximating the average helium temperature by weighting the average temperatures in five primary loop regions. Currently, the modeling of the steam generator cavity gas temperatures and their effect on loop pressure is very much simplified by assuming that the helium flow in the steam generator loop approaches zero soon after the initial transient and that the helium temperatures approach (exponentially) a nominal feedwater temperature thereafter. A depressurization option is also built in, allowing the loop pressure to decrease at a user-defined rate down to atmospheric after having reached the primary system relief-valve pressure limit setting. One could also build in assumptions of relief-valve cycling (rather than failing open) at the high-pressure limit. Partial depressurization scenarios can also be analyzed. These effects are modeled in subroutine PRESS.

### 3.2 CORE BYPASS FLOW MODELING

MORECA considers three core bypass paths: (1) a bypass stream heated by passing through the gaps between the reflector blocks, (2) a cold bypass which is assumed to pass (unheated) through the core barrel and enter the lower plenum and the steam generators, and (3) a cold bypass which avoids the core barrel and the steam generators entirely. The cold-flow bypass fractions and the split between the flows that enter and avoid the lower plenum are specified at the start, and the proportionality is assumed to be fixed throughout the run.

Depending on the initial conditions specified and how "trustworthy" they are thought to be, the user may want to specify some inputs and have others calculated. Those items that can be optionally specified as input data are

1. bypass fractions (initial),
2. total core power and flow,
3. radial peaking factors (RPFs) (axial peaking factors are specified in a data statement in the MAIN program),
4. initial element outlet temperatures,
5. entrance/exit pressure loss or effective orifice coefficients,
6. initial core pressure drop, and
7. steam generator helium inlet temperature.

If all of these parameters were input, the initial conditions would be overspecified. Therefore, a number of options are included to allow the user some choices. The input flags are FSQ (for flow skew) and TRUSTF (flag for "what to trust"). TRUSTF is set via a data statement in subroutine CFLOW. More details on input instructions for dealing with the bypass-flow modeling are given in Appendix B.

### 3.3 PLENUM MODELS

The plenum models used in the current MORECA code have evolved from the very detailed models originally developed in the ORECA code for the upper (core inlet) plenum and the lower (core outlet) plenum of both the FSV and large-HTGR designs. In uncontrolled core heatup accident (UCHA) transients, radiation heat transfer to the vessel is significant, and the variations in temperature between neighboring core regions can be large. Thus, a model was used to account for radiant heat exchange between individual plenum elements and core support blocks (upper and lower surfaces) and the cover plate areas (above or below) associated with individual regions. For example, in the upper plenum model, each element's upper surface exchanged heat with all of the opposing upper-plenum cover plates. Cover plates are modeled dynamically, that is, with their heat capacity included.

It was determined that radiant heat transfer to the side walls in both the upper and lower plenums was also important, so the modeling for radiant heat exchange between the plenum element surfaces and an "average-temperature" plenum sidewall was included. In this case, however, rather than having each region-to-sidewall heat exchange modeled, a weighted average temperature for each ring of elements was used. This approximation was justified on the basis that some smearing of the exchange will be done by the control rod drive tubes (upper plenum) or core support posts (lower plenum). The effects of these obstructions are not otherwise considered.

Two alternative models for calculating the radiant heat exchange in the plenums were tested in the ORECA code for the 2240-MW(t) HTGR design (Ref. 4). In the reference model, it was assumed that because the estimated emissivities and absorptivities are high (0.8), the effects of interreflected radiation within the chambers on the course of the accidents would be negligible (Ref. 10). In a more detailed model, an algorithm was used to include the total radiation heat exchange, accounting for the effects of multiple reflections among all surfaces in the plenums (Ref. 11). This model was also used for sensitivity studies involving effects of lower assumed values of emissivity and effects of "thermal polishing," in which the loss of the oxide coating on a hot surface can result in a significant decrease in emissivity (Ref. 12). Sensitivity tests showed that the differences between the two models were insignificant.

In the MORECA code (reference version), further simplifications were made by using concentric ring average approximations for radiant heat transfer between upper-plenum (and core support-block) surfaces and corresponding ring surfaces above (and below). Sensitivity studies using comparisons to the element-level model showed this to be a valid approximation. Details are given in Appendix A.

The upper-plenum heat transfer calculations are done in subroutine TOPTEM and the lower plenum in BOTTEM. The view factors for radiant heat transfer between the rings of elements, the upper and lower plenum surfaces, and the plenum sidewalls are generated in VFRING.

### 3.4 CORE BARREL AND VESSEL MODELS

The design of an optimum arrangement of heat shields and insulation protecting the vessel from the high temperatures of the core and the primary system coolant is not a straightforward optimization problem, and in fact involves several somewhat contradictory objectives. First, the insulation (thickness and location) design must account for both

operating conditions and accident conditions. Second, insulation should be reduced enough to allow for adequate heat transfer from a hot vessel to the RCCS to provide cooling for loss-of-forced-convection (LOFC) accidents, and at the same time it should be increased enough to keep the vessel temperatures from closely approaching or exceeding code limits. Third, in designing for heatup accident scenarios, there are significant differences in the locations of potential vessel hot points if the LOFC is pressurized (maximum temperatures in the upper vessel) or depressurized (maximum temperatures near the core barrel belt line), or even somewhere in between. Finally, the potential problem of vessel embrittlement from neutron bombardment needs to be considered because the vessel ductility is dependent on irradiation temperature. Because of all these factors, the modeling of the mechanisms contributing to vessel temperature predictions must be of sufficient accuracy to determine whether the design goals noted will be satisfied.

The core barrel and reactor vessel are each represented by 7 axial  $\times$  4 radial (quadrant) nodes, plus nodes corresponding to the regions opposite the inlet and outlet plenums. The "roof" and "floor" heat shields are each represented by seven concentric ring nodes. This is a simplification of previous (ORECA) reference models in which individual upper plenum cover-plate failures were of interest, and the roof model had a node to correspond to each upper reflector element surface. Cover-plate failure is not an issue here because the shields are made of a high-temperature material (Alloy 800) instead of carbon steel. Comparisons of heatup transient results using the more detailed plenum roof models show insignificant differences in predicted core temperatures. The heat transfer through the insulation resistance and radiation shielding of the upper-plenum insulation cover is also modeled explicitly.

### 3.5 REACTOR CAVITY COOLING SYSTEM MODEL

The Reactor Cavity Cooling System (RCCS) model incorporates detailed heat transfer and air natural circulation cooling calculations for panel nodes corresponding to adjacent vessel nodes. Independent flow and heat transfer (radiative and convection) equations for each of four quadrant panels allow simulation of the full range of expected performance and of degraded states including partial and total air passage blockage and system failures. A detailed report by J. C. Conklin on the RCCS model and its development is given in Ref. 13. In Conklin's report, the analysis and performance of the RCCS is decoupled from the reactor behavior by assuming that the reactor vessel node temperatures are fixed as boundary conditions. In MORECA, the vessel node temperatures are treated as variables dependent on the core and RCCS behavior. The current MORECA model simulates the PSID-design RCCS. Although design evolutions will be incorporated in future models, the performance characteristics of the RCCS (at least for air-cooled systems) are not expected to change significantly.

### 3.6 SHUTDOWN COOLING SYSTEM MODEL

The Shutdown Cooling System (SCS) consists of an auxiliary circulator and pressurized-water heat exchanger used for plant cooldown when the main circulator and steam generator are not available. The SCS is currently classified as a non-safety-grade system. Use of the SCS model is of particular interest for investigating scenarios in which

forced circulation flow is restored after long heatup periods during which no circulation was available. In some HTGR designs, this can become an operation-limiting situation because of the possibility of damage to metallic components downstream of the hot core outlet gases. The SCS inlet path has been designed to withstand such high temperatures, and MORECA calculations have shown that sufficient safety margins are available for all conceivable scenarios.

The SCS model in MORECA includes a steady-state thermal-hydraulic characterization of the auxiliary heat exchanger and a "flow-controlled" circulator model. Cooling water inlet temperature and flow are externally defined input functions. The helium flow rate through the SCS loop is user specified; an exception is that the SCS temperature control system, which reduces the helium flow if the heat exchanger coolant outlet temperature exceeds a specified limit, can alter the flow.

### 3.7 FUEL FAILURE MODELS

Currently, the MORECA code has two different fuel failure models built in. The first is a simple temperature-only failure dependence model in which the fraction of the total fuel that has at any time exceeded a user-specified fuel failure temperature is printed out periodically. A second, more detailed, fuel failure model has also been implemented that is based on a report by D. T. Goodin of GA (Ref. 14). This model predicts cumulative fuel failure (CFF) fractions that are dependent on the time the fuel spends at a given temperature. The failure rate is a function of two effects, a nonlinear mechanism caused by decomposition and diffusion and a linear mechanism caused by corrosion and diffusion. Because of the nonlinear dependence of the CFF on time at a certain temperature, the original Goodin equations had to be approximated by a linear model to accommodate effects of time at temperature; it assumes that failures are independent of fuel age or burnup. This fuel failure model was developed for the larger HTGRs, which did not have the same degree of passive safety as the MHTGR and thus had relatively large predicted fuel failure fractions for the beyond-design-basis accidents, where maximum fuel temperatures far exceeded 1600°C. For the accident scenarios covered in this report, no fuel failure is reported, because the predicted maximum fuel temperatures were not high enough to cause failure fractions above the normal background levels, at least for the currently used models.

Another fuel failure model has been developed from later Goodin work, which provides more accurate results in the lower temperature, lower failure rates regimes, and would be more applicable to the MHTGR (Ref. 15). Additional fuel failure modeling efforts by DOE germane to the MHTGR are currently under way, and updated models are expected to be incorporated into MORECA in the near future.

#### 4. SUMMARY OF MORECA RUNS, CAPABILITIES, AND FINDINGS

There are two general classes of heatup accidents studied using the MORECA code in which the RCCS is assumed operational. The first is the rapid depressurization and immediate Loss of Forced Circulation (LOFC) with scram, with no subsequent primary coolant system forced cooling. This case corresponds to the SRDC-11 case in the PSID. In the reference case, depressurized LOFC calculation (Fig. 2), peak temperatures are reached after 4–5 days. There is no fuel failure, because the maximum peak fuel temperature [1482°C (2699°F)] is well below the 1600°C nominal "limit." The maximum vessel temperature [478°C (893°F)] is below the 538°C (1000°F) extended code limit for a depressurized vessel. These results are generally in good agreement with PSID values except for vessel temperatures, where the PSID's maximum was less than 427°C (800°F). Reasons for this discrepancy are being investigated.

The second class of heatup accident with RCCS operational is the pressurized LOFC with scram, which corresponds to the DBE-1 case in the PSID. Results are shown in Fig. 3. The maximum fuel temperatures predicted are even lower than those in the depressurized LOFC case, and concern for any fuel damage is nil. The primary concern is for vessel temperature [maximum 469°C (876°F)], which exceeds the 427°C (800°F) extended code limit for a pressurized vessel. The corresponding PSID prediction, using the GA PANTHER code, was 400°C (750°F). Some of the discrepancies were found to be due to simplifications in the PANTHER code that GA plans to address in the next stages of the design; however, some others have not yet been resolved. As in the PSID calculation, the MORECA prediction of maximum primary system pressure [7.05 MPa (1022 psia)] was not high enough to actuate the relief valve [7.18 MPa (1041 psia)]; however, the MORECA assumptions of steam generator cavity temperatures, which have a significant effect on pressure, were quite simplified and arbitrary. The extent of the overtemperature at pressure predicted here would not be expected to cause a vessel failure; however, considering the uncertainties involved in the temperature predictions, means should be provided to depressurize, and vessel temperature monitoring should be provided. Monitoring would provide a basis for regulators to judge whether restart following an LOFC should be allowed.

##### 4.1 ACCIDENT SCENARIO SENSITIVITY STUDIES

Many variations of the two classes of LOFC accidents were studied to observe sensitivities of the severity of the predicted results to both parametric (modeling) and operational assumptions.

Of the many parametric variations in the "reference" depressurized and pressurized LOFC cases, three were found to be of major significance in determining the safety-related outcome of the predictions: (1) assumptions of fuel and reflector thermal conductivities; (2) use of the conservative (PSID) afterheat relationship vs the "best estimate" curves; and (3) variations in assumed RCCS performance including effects of assumed emissivity values that have a direct effect on transfer of heat from the core blocks to the RCCS panels.

The reference case assumption for reflector conductivity is that only the central reflector and first ring of elements surrounding the fuel suffer significant radiation damage (along with the fuel itself). However, for the case of relatively unirradiated (or annealed)

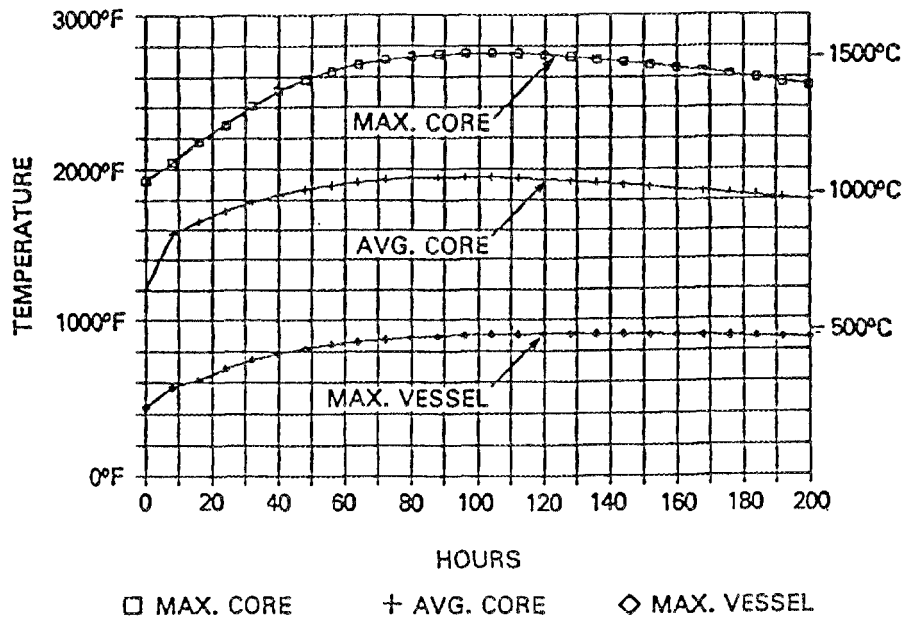


Fig. 2. Reference case depressurized loss of forced convection accident with reactor cavity cooling system operational, temperatures of core and vessel vs time.

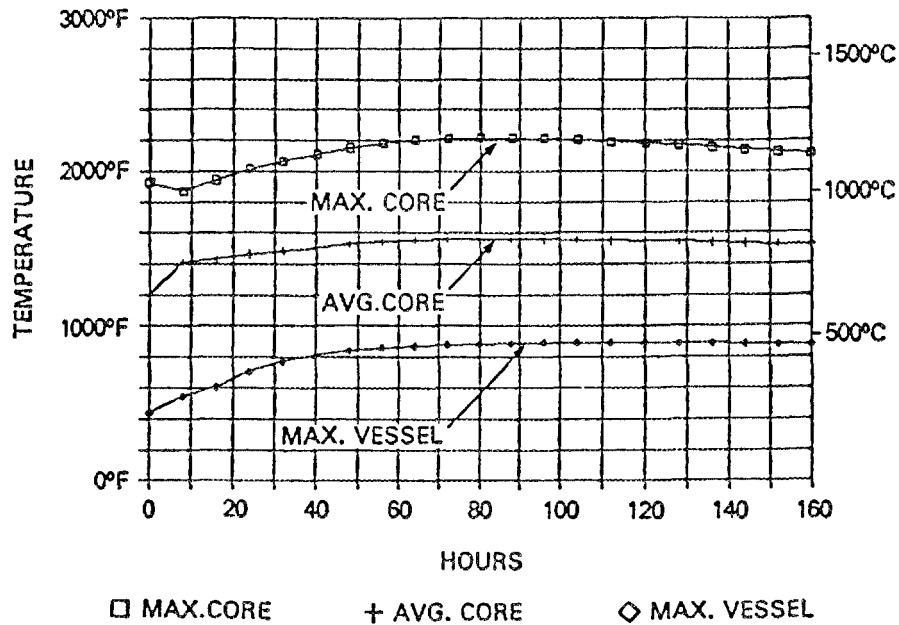


Fig. 3. Reference case pressurized loss of forced convection accident with reactor cavity cooling system operational, temperatures of core and vessel vs time.

elements, the thermal conductivities would be considerably higher. Data on effective fuel and graphite conductivities are typically difficult to quantify because of effects of impurities, geometries, gaps, thermal radiation effectiveness, and annealing that may take place during measurements. Hence, we have assumed that there may be wide variations in the core conductivity values, due both to data uncertainties and to actual changes due to the operating history.

Typically, increasing the fuel and outer reflector conductivities will enhance heat transfer to the RCCS heat sink in LOFC heatup accidents, resulting in lower peak fuel temperatures. Results showed that several-hundred-degree variations in peak fuel temperatures were possible due to reasonable variations in assumed conductivities. Although the "low end" values of core conductivity were used in the reference case (resulting in acceptable peak fuel temperatures for the limiting-case depressurized LOFC), it is seen as essential that the conductivity relationships be carefully verified to provide assurance of negligible fuel failure.

The maximum vessel temperature prediction is also affected by core thermal conductivity assumptions. Although it was expected that increased core conductivities would result in higher peak vessel temperatures, in fact the opposite was true, at least for the cases where the axial conductivity was assumed to increase along with the radial. Increased conductivities (favorably) changed the times at which the peak temperatures occurred and made the core temperatures more uniform (axially and circumferentially), thus reducing the gradients.

Use of the "best estimate" afterheat curve (vs the reference case, considerably more conservative PSID relationship) results in predicted peak fuel temperatures about 150 to 250°C lower for the depressurized LOFC (depending on other parameter assumptions). There is less of an effect for the pressurized cases. Peak vessel temperatures for the best estimate afterheat cases are typically about 50°C lower. Use of the Fort St. Vrain FSAR afterheat curve gives results nearly identical with those that use PSID values.

Although the performance of the RCCS during postulated heatup accidents has relatively little effect on peak fuel temperatures, it can have a significant effect on peak vessel temperatures. For example, for a depressurized LOFC in which the RCCS was assumed to be failed totally for a one-day period after the LOFC and scram, the maximum fuel temperature increase was less than 20°C greater than the case of no RCCS failure. Assuming emissivity values of 0.5 (vs 0.8 in the reference case) for the RCCS panels and vessel walls increases the predicted peak fuel temperature in depressurized LOFCs by only about 30°C, but the peak vessel temperature increases by about 120°C. Hence, it is important that the critical emissivity values be maintained in the 0.8 range. In depressurized LOFCs where air flow in one of the four quadrant RCCS panels is substantially blocked (friction factor times 200), the maximum fuel temperature goes only about 10°C higher than without the blockage. The temperature of the section of vessel opposite the failed panel, however, will exceed its design limit in one to two days. Hence, the RCCS performance monitoring should be able to detect partial RCCS failures (especially for pressurized LOFCs) so that suitable corrective actions (such as depressurization) could be taken.

Besides the three most important variations noted, many other variations such as the following were studied which were all shown to have only minor effects on the safety-related outcome of the accidents.

1. An arbitrary cooldown period following the scram, which makes the effective "initial condition" temperatures of the core lower or, conversely, an assumption of arbitrarily

degraded RCCS panel performance for a relatively short period following the scram, increasing the "initial" core temperatures. Although these variations had only a relatively small effect on maximum fuel temperatures, localized or intermittent failures in the RCCS heat removal function had significant (detrimental) effects on maximum vessel temperatures.

2. Variation in the assumed initial reflector bypass flow fraction, as noted previously. In earlier MORECA calculations of pressurized LOFCs in which thermal insulation in the upper vessel region was omitted, a large (~10%) assumed bypass flow resulted in significantly higher maximum vessel temperatures, compared with assuming no bypass flow (as is done in the PSID). However, after adding the insulation, the maximum vessel temperatures for the pressurized LOFC appeared in the area adjacent to the fuel, and assumed bypass flow fraction variations had little effect on maximum vessel temperature. Maximum fuel temperatures are affected by bypass flow but stay well below failure limits in all cases.
3. Variation in the assumed initial and shutdown peaking factors, both axially and radially. This variation addresses the difference between the power distribution during operation (as given in the PSID and as used in the reference calculations even after a scram) and the power distribution that is "smeared" out considerably, which more realistically models postscram gamma heating. An interesting aspect of this particular sensitivity study was that in the pressurized LOFC case where a uniform postscram power distribution was assumed, the nonuniform azimuthal temperatures persisted throughout the accident as a result of the initial nonuniform fuel temperatures and natural convection flow patterns set up at the start.
4. Variations in RCCS flow loss coefficients (i.e., for increased friction factors or partial blockage) and air side heat transfer coefficients. Variations over relatively wide ranges had minor effects on RCCS heat removal performance.
5. Variations in the correlations used to predict helium-to-fuel heat transfer. Over the uncertainty ranges for these correlations, at-power (turbulent flow) coefficient variations have minor effects on fuel temperatures relative to the (large) margins between operating and fuel failure temperatures. For low-flow, shutdown cases (laminar and transition regimes), sensitivity studies have shown that maximum temperatures are very insensitive to heat transfer coefficient because the gas temperatures closely approach the fuel temperatures anyway.
6. Variations in outdoor temperature (RCCS inlet air temperature). The reference case assumed 29°C (85°F), while the maximum design temperature is 43°C (110°F). Peak vessel temperatures increase about one degree for every two-degree rise in ambient.

## 4.2 COMPLETE RCCS FAILURE

A "complete" failure of the RCCS is currently seen as a nonmechanistic failure because no reasonable total failure mechanisms have been postulated. In the current calculation, the RCCS structure with its insulation between the riser and downcomer is

assumed to be in place, but there is no air flow. Conduction and thermal radiation to the concrete silo is modeled simplistically, and credit is taken for the concrete heat capacity. No credit is taken for heat losses to the upper and lower heads. The results are shown in Fig. 4. Although the peak fuel temperature of 1606°C (2923°F) exceeds the 1600°C "limit," the predicted fuel failure is insignificant. The maximum vessel temperature, however, exceeds code values in about one day, and reaches dangerously high temperatures within two to four days.

#### 4.3 INTERACTIVE WORKSTATION VERSION OF MORECA

With the SUN workstation version of MORECA, it is possible for the operator/analyst to have direct on-line involvement with the postulated accident scenarios. The workstation display screen (Fig. 5) has a middle section in which the summary status of the simulation is presented for the RCCS, vessel, core, and SCS. Along the bottom of the screen are the "buttons" (accessed by a mouse) allowing operator intervention including control of the simulation speed, control of the SCS parameters, allowance for "degrading" the effectiveness of the RCCS, and control of total or partial depressurization transients. The maximum vessel and core temperatures are displayed at elevations corresponding to their occurrence. This display feature is expected to be useful for review and confirmation studies of the safety system design, operator emergency procedures, operator training procedures, and postaccident monitoring systems.

#### 4.4 CONCLUSIONS

From the LOFC heatup accident analyses, it is evident that the current MHTGR design is not susceptible to significant fuel failure from postulated accidents even from very low probability or even from certain drastic, nonmechanistic events. The ORNL results generally corresponded well with independent calculations by DOE contractors and by BNL. Considering that these are calculations of some of the most serious types of accidents that can be reasonably postulated, the fact that there is such good general agreement indicates that the analyses are relatively straightforward and therefore credible. The one major area of concern was with possible vessel overheating, and that would not be considered an immediate safety concern unless RCCS or partial RCCS failures occurred. Sensitivity studies showed that the most crucial safety-related parameter or operational uncertainties were the core thermal conductivities, the afterheat function, and the effective RCCS heat removal performance.

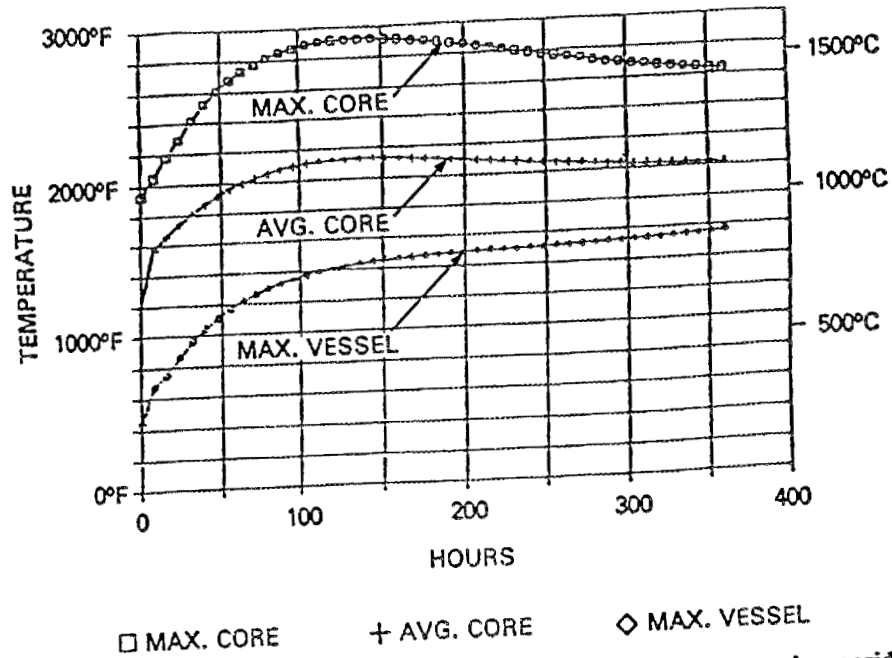


Fig. 4. Reference case depressurized loss of forced convection accident with reactor cavity cooling system not operational, temperatures of core and vessel vs time.

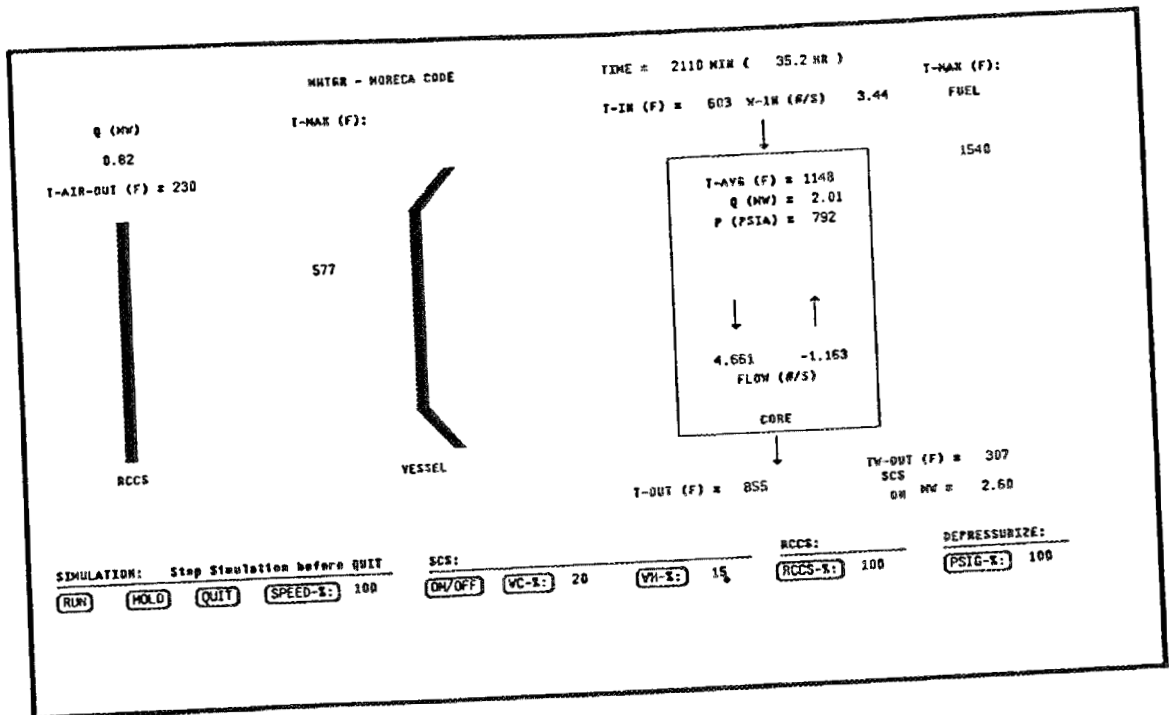


Fig. 5. MORECA Interactive workstation version accident scenario display screen.

## 5. REFERENCES

1. S. J. Ball, *ORECA-I: A Digital Computer Code for Simulating the Dynamics of HTGR Cores for Emergency Cooling Analyses*, ORNL/TM-5159, Oak Ridge National Laboratory, Oak Ridge, Tenn., 1976.
2. R. M. Harrington et al., "HTGR Severe Accident Sequence Analysis," *Proceedings of the Third Japan-U.S. Seminar on HTGR Safety Technology*, BNL-NUREG-51674, Brookhaven National Laboratory, Upton, N.Y., 1982.
3. S. J. Ball et al., "Safety and Licensing Analyses for the Fort St. Vrain HTGR," *Proceedings of the Third Japan-U.S. Seminar on HTGR Safety Technology*, BNL-NUREG-51674, Brookhaven National Laboratory, Upton, N.Y., 1982.
4. H. J. Reilly et al., *Preliminary Evaluation of HTGR Severe Accident Source Terms*, EGG-REP-6565, Idaho National Engineering Laboratory, Idaho Falls, 1984.
5. S. J. Ball, "Dynamic Model Verification Studies for the Thermal Response of the FSV HTGR Core," *Proc. 4th Power Plant Dyn., Control, Test. Symp.*, The University of Tennessee, Knoxville, 1980.
6. S. J. Ball and J. C. Conklin, "Modular HTGR Simulation Using Parallel Processors," *Proc. 7th Power Plant Dyn., Control, Test. Symp.*, The University of Tennessee, Knoxville, 1989.
7. P. M. Williams et al., *Draft Preapplication Safety Evaluation Report for the Modular High-Temperature Gas-Cooled Reactor*, NUREG-1338, U.S. Nuclear Regulatory Commission, 1989.
8. A. J. Neylan, "MHTGR Heat and Mass Transfer Data", GA/NRC-006-86, General Atomics, San Diego, letter to T. L. King, U.S. Nuclear Regulatory Commission, April 3, 1987.
9. U.S. Department of Energy, *Preliminary Safety Information Document for the Standard MHTGR*, Updates Through Amendment 10, HTGR-86-024, 1989 (this document is classified as "Applied Technology" and is not available to the public domain; requests for this document should be made through the U.S. Department of Energy, Washington, D.C.).
10. W. H. Giedt, Chap. 13 in *Principles of Engineering Heat Transfer*, Van Nostrand, Princeton, N.J., 1961.
11. J. C. Conklin, *Development and Adaptation of Conduction and Radiation Heat Transfer Codes for the CFTL*, ORNL/TM-7854, Oak Ridge National Laboratory, Oak Ridge, Tenn., 1981.
12. U. Gat and P. R. Kasten, *Gas-Cooled Reactor Program Annual Progress Report for Period Ending December 31, 1977*, pp. 11-15, ORNL-5426, Oak Ridge National Laboratory, Oak Ridge, Tenn., 1978.

13. J. C. Conklin, *Modeling and Performance of the MHTGR Reactor Cavity Cooling System*, ORNL/TM-11451, Oak Ridge National Laboratory, Oak Ridge, Tenn., 1990.
14. D. T. Goodin, *Accident Condition Performance of HTGR Fuels*, A-16508, General Atomics, San Diego, 1983.
15. D. T. Goodin, *Fuel Failure Model for MHTGR*, HTGR-85-107, Rev. 1, U.S. Department of Energy, 1985.

**Appendix A**

**DETAILED MODEL DESCRIPTIONS**



## A.1 FUEL AND REFLECTOR ELEMENT BLOCK CONDUCTION MODELING

A single-node representation of the temperature and the energy storage in a large hexagonal graphite block fuel element (Fig. A.1) could not accurately portray the large fuel-to-moderator temperature differences that exist at full-power conditions. It would also preclude approximating the at-power reactivity feedback for the neutron kinetics equations because the individual effects of fuel and moderator temperature changes are not modeled. However, for studies of shutdown power and flow scenarios, for which MORECA is primarily intended, the radial temperature gradients within the block are reduced to small values within a few minutes after shutdown, and the reactivity effects are no longer significant after the reactor is scrammed.

The question remains, however, as to how accurately the single-node-per-element model can be used to predict the temperature transients. In general, the accuracy of any finite-differencing scheme for modeling diffusion decreases as the frequency content of the perturbation increases; and, for heat conduction models, the grosser the mesh size, the more the transient heat flux between nodes is underestimated (Ref. A.1). In most cases, an underestimation of heat flux between adjacent elements will yield conservative (i.e., higher-than-actual) hot fuel-element temperatures.

A rough approximation of the accuracy of the one-node-per-element mesh can be derived by use of a method developed by the author (Ref. A.1) to determine the ratio of approximate-to-actual heat flux for slab geometry perturbation frequency. The dimensionless perturbation frequency  $\Omega$  is defined by

$$\Omega = \frac{(\Delta X)^2 \omega}{2D_H} , \quad (\text{A.1})$$

where

$$\begin{aligned} D_H &= k/\rho C_p = \text{composite core heat diffusivity, } \approx 0.006 \text{ ft}^2/\text{min}; \\ \omega &= \text{perturbation frequency, radians/min}; \\ k &= \text{conductivity, Btu/(h}\cdot\text{ft}\cdot^\circ\text{F)}; \\ \rho &= \text{density, lb/ft}^3; \\ C_p &= \text{specific heat, Btu/(lb}\cdot^\circ\text{F)}; \\ \Delta X &= \text{node thickness, ft.} \end{aligned}$$

To "translate" an accident transient into a perturbation frequency, we note that because typical MHTGR loss of forced convection and depressurization accident analyses show that peak core temperatures occur in no less than 10 h after the initial failures, a complete (sinusoid) cycle would occur in <40 h, so an equivalent maximum perturbation frequency would be 0.025 cycle/h, or  $\sim 0.003$  radian/min. The corresponding  $\Omega$  value [Eq. (A.1)] is  $\sim 0.4$  which, referred to Fig. 2 of Ref. A.1, indicates that the radial heat flux between neighboring regions is underestimated by only a few percent at this frequency. In other words, one might arbitrarily increase the interregion radial conduction by 2–3% to obtain more accurate results for typical heatup accidents.

Another means of determining the transient accuracy of the finite-difference core conduction model is to compare model transient results with those of finer mesh approximations. This was done for the original ORECA model, where each node was a

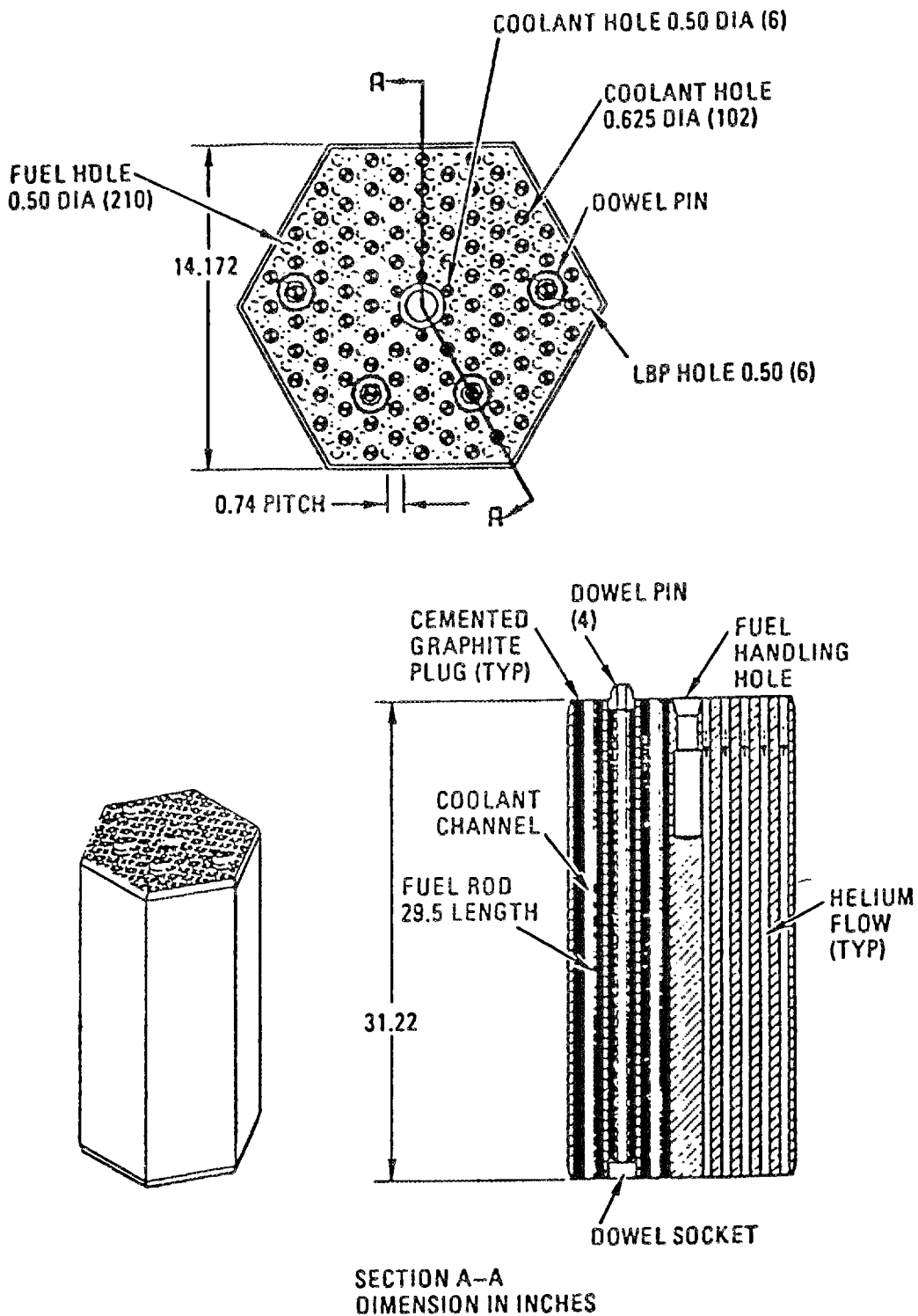


Fig. A.1. Standard fuel element. Source: U.S. Department of Energy, *Preliminary Safety Information Document for the Standard MHTGR*, HTGR-86-024, Vols. 1-5, 1986, plus ten amendments through February 1989 (this document is classified as "Applied Technology" and is not in the public domain; requests for this document should be made through the U.S. Department of Energy, Washington, D.C.).

seven-element "region" or cluster (Ref. A.2). In that case, it was concluded that a 50% increase in effective radial conductivity would compensate for the large mesh size. Those studies also showed that for perturbation frequencies of interest, errors in temperature calculations incurred from using one node per fuel element were negligible.

From the preceding arguments, we concluded that no conductivity enhancement was warranted for the MORECA core modeling.

The effective radial conductance between elements is accounted for by the geometric factor in the conduction equation. This is treated very simply (and arbitrarily) in the MORECA code, as it was in ORECA. Noting that in hexagonal geometry each block has six radial neighbors instead of four, as in slab or square-prism geometry, the equivalent slab geometric conductance term  $G_{\text{slab}}$  needs to be multiplied by 4/6:

$$G_{\text{slab}} = \frac{\text{mean area}}{\text{characteristic length}} = \frac{A}{\Delta X} \approx \frac{DL}{D} = L \quad , \quad (\text{A.2})$$

where  $D$  is the distance across flats of a hexagonal element (1.181 ft), and  $L$  is the length of a block (2.602 ft).

Therefore, the heat transfer rate  $Q$  (Btu/h) between radially adjacent element blocks with the difference between mean temperatures  $\Delta T$  is determined from

$$Q = \frac{4}{6} G_{\text{slab}} k' \Delta T \quad , \quad (\text{A.3})$$

where  $k'$  is the effective conductivity, Btu/(h·ft·°F).

The usual form of the energy balance equation for node  $(i, j)$  is

$$\begin{aligned} \rho A \Delta X C_p \frac{dT_{ij}}{dt} = M C_p \frac{dT_{ij}}{dt} = \frac{k'A}{\Delta X} [(T_{i+1,j} - T_{ij}) + (T_{i-1,j} - T_{ij}) + \dots] \\ + \frac{k_a A_a}{L} [(T_{i,j+1} - T_{ij}) + (T_{i,j-1} - T_{ij})] = Q_{ije} \quad , \end{aligned} \quad (\text{A.4})$$

where  $T_{i+1,j}$ ,  $T_{i-1,j}$ , etc., are the temperatures of its radial neighbors, °F;  $T_{i,j+1}$  and  $T_{i,j-1}$  are temperatures of its axial neighbors, °F;  $Q_{ije}$  are the heat inputs to node  $i$  from internal heat generation and convection, Btu/h;  $M$  is the mass of the element, lb;  $i$  is a subscript denoting radial position; and  $j$  is a subscript denoting axial position.

The effective conductivity terms  $k'$  and  $k^a$  are dependent on four different parameters: node average temperature, type of material (fuel or reflector), geometry and orientation (radial or axial), and irradiation history. Conductivities are calculated for each node at each time step in function routines RADK (radial) and AXIK (axial). The heat transfer between node  $(i,j)$  and all of its neighbors could be approximated by multiplying this value of  $k'$  by the summation of the temperature differences; however, because rather large differences in neighboring  $k'$  values can exist, this would lead to heat-balance errors due to significant differences between the calculations of heat transfer in and out. Hence, an average global effective conductivity term for each node is calculated at each time step which accounts for its own and all its neighbors' effective conductivities. Then the temperature differences between the node and each neighbor are multiplied by the ratio of the average  $k'$  for those two nodes to the global average. These calculations are done in subroutine ALGEN. This technique permits the use of the efficient core heat transfer

solution (Sect. A.10) and has been tested and shown to give accurate heat balances for conduction-dominated transients.

An option flag (KCH) set in routines RADK and AXIK allows the user a choice of FSV-FSAR or updated [General Atomics (GA) proprietary] MHTGR values of conductivity. The public-domain FSV expressions for conductivity, which are generally conservative (low) and do not include differences due to irradiation histories, are simple linear functions of temperature, corrected for node geometry differences.

The specific heat terms for the composite core and reflector elements are also included as functions of temperature and are calculated in subroutine TPROP. Thus, strictly speaking, the  $MC_p dT_{ij}/dt$  term in Eq. (A.4) should be  $(M) dh/dt$ , where  $h$  is the specific enthalpy. However, because  $C_p$  is defined (for small changes in temperature) as  $dh/dt$ , the expression for  $C_p$ , evaluated at the node temperature, can be used in Eq. (A.4): because  $C_p$  is defined (for small changes in temperature) as  $dh/dt$ , the expression for  $C_p$ , evaluated at the node temperature, can be used in Eq. (A.4):

$$C_p[\text{Btu}/(\text{lb}\cdot^\circ\text{F})] \approx 0.115 + 0.34(1.0 - e^{-T/960}) \quad (\text{fuel element}) \quad , \quad (\text{A.5})$$

where  $T$  is the core node temperature,  $^\circ\text{F}$ . Values of effective  $C_p$  for other core elements are proportional to those for the fuel elements and account for differences in the element's average density and size.

## A.2 INTERNAL HEAT GENERATION CALCULATIONS

The internal heat generation  $Q_{ij}$  in the refueling region node ( $ij$ ) is an independent input function of time:

$$Q_{ij} = Q_{AIO} QR_i QA_j Q(t) \quad , \quad (\text{A.6})$$

where  $Q_{AIO}$  is the average initial core heat generation rate,  $QR_i$  is the radial power factor for radial position  $i$ ,  $QA_j$  is the axial power factor for axial position  $j$ , and  $Q(t)$  is the fraction of initial power vs time.

$QA_j$  and  $QR_i$  values, which determine the power shaping, are input by means of data statements and input deck values (respectively) and are assumed constant.  $Q_{AIO}$  is an input number that is determined from the overall core power density. For an example calculation of  $Q_{AIO}$ , consider a case starting from 100% power (350 MW). The average core power density is 5.9 kW/L, with 99% of the power assumed to be generated in the active core and the rest in the reflectors. Hence, the average initial power for a fuel element column is

$$Q_{AIO} = \frac{(350)(0.99)}{66} = 5.25 \text{ MW} \quad .$$

The calculation of average element power generation by the preceding method is significantly lower than the average (composite fuel + moderator) power densities typically derived from a single fuel pin (or coolant channel) geometry model (Ref. A.3). The reason is that the local geometry in a fuel-coolant reference "cell" is not typical of the overall core; in fact, the power density in this cell is  $\sim 30\%$  higher than the average power

density in a standard fuel element and ~34% higher than the active core average. While the local cell model is appropriate for high-coolant flow cases (where the heat convection term is the dominating heat transfer mechanism), it is not an accurate model for shutdown transients where the overall core heat capacity dominates the response.

Treatment of the reflector blocks is similar to that of the active core block. The power fraction vs time in the side reflector blocks,  $Q_{SR}(t)$ , is assumed to have the same shape as  $Q(t)$  for the core. This is conservative as long as the only induced activity is that due to carbon-14.

### A.3 CORE CONVECTION HEAT TRANSFER MODELING

Because the flow in the coolant channels varies over a wide range in emergency cooling situations, it is necessary to consider all three flow regimes (turbulent, transition, and laminar) and upflow as well as the normal downflow direction. The "standard" Dittus-Boelter heat transfer correlation was approximated for the turbulent regime as follows:

1. Turbulent ( $Re \geq 4000$ ):

$$h = (0.023)(0.88) \frac{k}{D} (Re)^{0.8} , \quad (\text{A.7})$$

where

$h$  = heat transfer coefficient from gas to fuel element block, Btu/(h·ft<sup>2</sup>·°F);

(0.88) = approximately the 1/3 power of the Prandtl number for helium in the range of interest;

$k$  = conductivity of helium, Btu/(h·ft·°F);

$D$  = coolant channel diameter, ft;

$Re$  = Reynolds number,  $DG/\mu$ ;

$G$  = helium mass flow per unit area lb/(ft<sup>2</sup>·h);

$\mu$  = helium viscosity, lb/(ft·h).

2. Laminar ( $Re \leq 2100$ ):

For laminar flow, the average value for  $h$  over the length,  $L$ , of a channel was derived from Ref. A.4:

$$h = \frac{2k}{D} \left( \frac{WC_p}{kL} \right)^{0.333}, \quad (\text{A.8})$$

where

$W$  = channel flow rate, lb/h,  
 $C_p$  = helium specific heat, 1.241 Btu/(lb·°F),  
 $L$  = length of channel, ft.

### 3. Transition ( $2100 < Re < 4000$ ):

The value of  $h$  is computed as a linear function of the Reynolds number between the values of  $h$  (laminar) at  $Re = 2100$  and  $h$  (turbulent) at  $Re = 4000$ .

The physical properties of helium are approximated by:

$$k \approx 0.09 + 7.67 \times 10^{-5} \bar{T}, \quad (\text{A.9})$$

and

$$\mu \approx 0.054 + 4.125 \times 10^{-5} \bar{T}, \quad (\text{A.10})$$

where, instead of the average helium temperature, the adjacent block temperature  $\bar{T}$  is used as an approximation ( $\bar{T}$  is in °F). As noted in the report (Sect. 4.1, Accident Scenario Sensitivity Studies), the safety significance of the results are not sensitive to the expected range of uncertainties in the heat transfer correlations, including the Reynolds number flow regime transition points.

The calculation of the heat exchanged between a solid node and a coolant gas can be approximated in a variety of ways. When the solid is represented as a point mass at temperature  $T_s$  (assumed to be uniform over the node), the heat transferred from solid to coolant,  $Q_{sc}$ , is often calculated by

$$Q_{sc} = hA(T_s - \bar{T}_c). \quad (\text{A.11})$$

An arithmetic average coolant temperature  $\bar{T}_c$  can be used, that is,

$$\bar{T}_c = \frac{T_{ci} + T_{co}}{2}, \quad (\text{A.12})$$

where  $T_{ci}$  and  $T_{co}$  are the coolant inlet and outlet temperatures, and  $T_{co}$  is determined from

$$Q_{sc} = WC_p(T_{co} - T_{ci}). \quad (\text{A.13})$$

However, this approach may seriously overestimate the amount of heat transfer and give values of  $T_{co}$  greater than  $T_s$  (when the gas is being heated), especially at low flow rates. It can also result in a "wrong-way" response to rapid changes of the inlet coolant temperature. To avoid these (nonphysical) situations, the value of the quantity ( $hA/WC_p$ )

must be  $\leq 2.0$ . (Ref. A.1). Because this often cannot be achieved for very low dimensionless characteristic length flows, the "end point weighing" (EPW), or "well-mixed" approximation, is sometimes used (such as is assumed in the RECA code, Ref. A.5). In the EPW approximation the mean temperature of the coolant is assumed equal to the outlet temperature, that is,  $T_c = T_{co}$ . This avoids both the overestimation of the heat transferred and the wrong-way response problem, but in the general case of slug flow, it underestimates the heat transfer rates over the entire flow range. Also, for initial full-power conditions, it overestimates the stored energy and peak fuel temperatures in the core.

The model for heat exchange from the coolant to the adjacent solid node used in the MORECA code is known as the "exponential approach" method, where

$$T_{co} = T_{ci} + (T_s - T_{ci})(1 - e^{-hA/WC_p}) \quad . \quad (A.14)$$

This model gives an "exact" solution for the heat transfer rate for the case where the solid temperature is assumed to be uniform over the entire length of the node, the coolant transit time is negligible, and the physical properties are constant. It also avoids the wrong-way response problem. A comparison of the steady-state values of percent approach vs  $(hA/WC_p)$  for the arithmetic mean, EPW, and exponential approach models is shown in Fig. A.2.

The percent approach concept, commonly used in heat exchanger design characterization, is defined as

$$\% \text{ approach} = 100 \left( \frac{T_{co} - T_{ci}}{T_s - T_{ci}} \right) \quad . \quad (A.15)$$

Figure A.2 clearly shows the underestimation of heat transfer by the EPW method and the errors incurred from using the arithmetic average.

#### A.4 FUEL ELEMENT FLOW RATE EQUATIONS

Unlike the Fort St. Vrain reactor and later designs of large HTGRs, MHTGR fuel element flows cannot be adjusted by an inlet orifice valve. Hence, the flow distributions are governed by the temperature-dependent flow resistance, which in turn depends on element peaking factors. Over the operating power and flow range, the element-by-element flows are approximately proportional to the total core flow rate. However, with temporary flow stoppages and with low flows typical of emergency cooling situations, the region flow distribution becomes quite sensitive to temperature effects, buoyancy forces, and other factors and are thus very important in determining maximum fuel temperatures. Hence, one must solve for all of the element flows simultaneously to determine any one of them.

The element flow equation in MORECA is very similar to its counterpart in RECA. It is a one-dimensional momentum equation for incompressible flow in a channel and is applicable to all cases of interest except during periods of very rapid depressurization:

$$\Delta P = W_i^2 \left( \frac{R}{g_c A^2 P} \right) \left[ K_i T_{IP} + \sum_{j=1}^{NA} T_{0ij} - T_{ij} + \frac{2fL}{D} \frac{1}{T_{ij}} \right] - \frac{gLP}{g_c R} \sum_{j=1}^{NA} \frac{1}{T_{ij}} \quad , \quad (A.16)$$

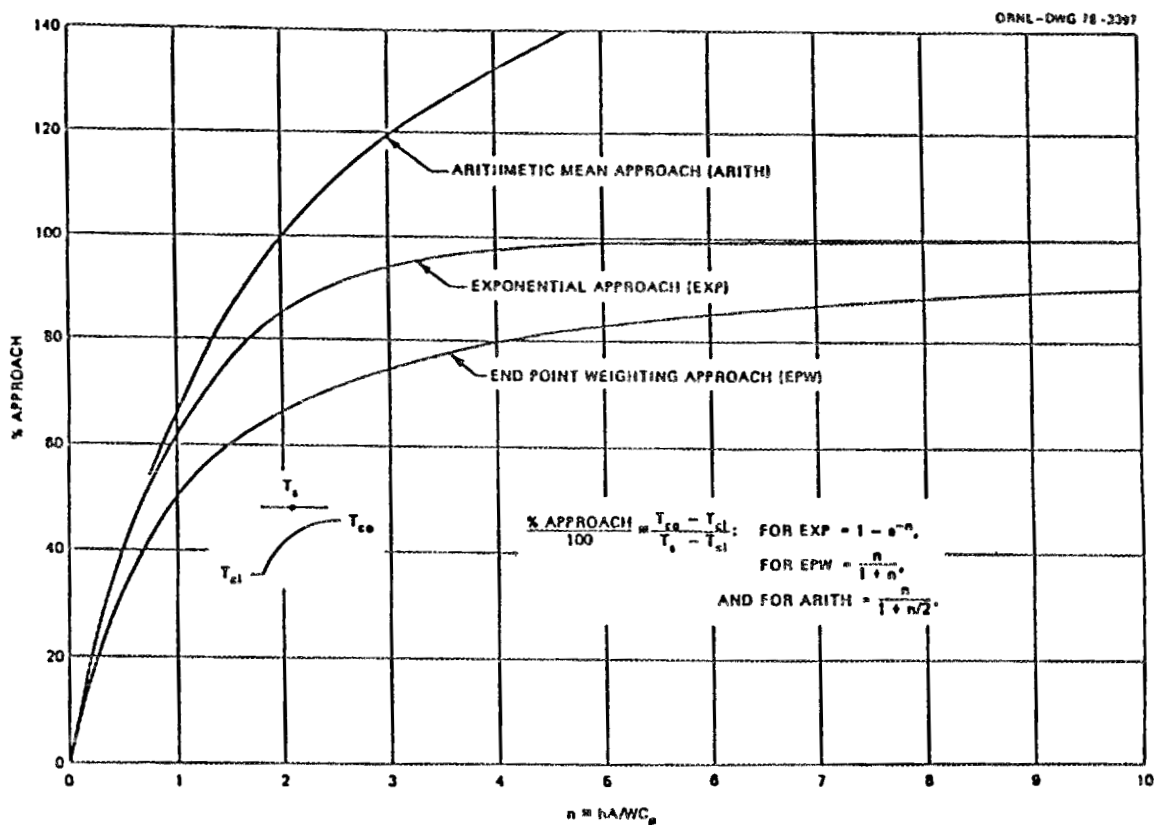


Fig. A.2. Comparison of coolant heat transfer methods.

where

- $\Delta P$  = core plenum-to-plenum pressure drop,  $\text{lb}_f/\text{ft}^2$ ;
- $W_i$  = channel  $i$  flow rate,  $\text{lb}_m/\text{s}$ ;
- $R$  = gas constant for He,  $386 \text{ ft}/(\text{lb}_f \cdot \text{R} \cdot \text{lb}_m)$ ;
- $g$  = acceleration due to gravity,  $32.2 \text{ ft}/\text{s}^2$ ;
- $g_c$  = conversion factor,  $32.2 \text{ ft}/(\text{lb}_m \cdot \text{s}^2 \cdot \text{lb}_f)$ ;
- $A$  = fuel element cross section area,  $\text{ft}^2$ ;
- $P$  = average channel pressure,  $\text{lb}_f/\text{ft}^2$ ;
- $K_i$  = lumped resistance coefficient for inlet flow distribution and other restrictions;
- $T_{IP}$  = inlet plenum temperature,  $^{\circ}\text{R}$ ;
- $j$  = index of axial element;
- $NA$  = number of axial elements;
- $T_{0j}$  = outlet temperature, element  $ij$ ,  $^{\circ}\text{R}$ ;
- $T_{ij}$  = inlet temperature, element  $ij$ ,  $^{\circ}\text{R}$ ;
- $f$  = Fanning friction factor;
- $L$  = axial element length,  $\text{ft}$ ;
- $D$  = mean hydraulic diameter,  $\text{ft}$ ;
- $\bar{T}_{ij}$  = average temperature, element  $ij$ ,  $^{\circ}\text{R}$ .

The temperature difference terms ( $T_{0ij} - T_{ij}$ ) account for the losses due to acceleration; the friction factor,  $f$ , is a function of flow regime and the summation term on the right-hand side is the buoyancy, or static head, term.

The friction factor,  $f$ , in the turbulent region ( $Re > 4291$ ) is approximated by

$$f \approx 0.0014 + 0.125 Re^{-0.32} \quad (\text{A.17})$$

and in the laminar region ( $Re \leq 1600$ ) by

$$f \approx \frac{16}{Re} \quad (\text{A.18})$$

In between these two regions,  $f$  is assumed to be constant at 0.01. Sensitivity studies to determine the effects of assuming higher friction factors and splitting the entrance and exit loss terms (rather than lumping them at the inlet) show that, in general, these considerations have little effect on the maximum predicted temperatures.

MORECA assumes that the total core flow  $\sum W_i$  is specified as an input function and then uses an iterative scheme to find the "correct" overall core  $\Delta P$  to satisfy the total flow conditions.

## A.5 PLENUM MODELS WITH RADIATION HEAT TRANSFER

While detailed models were used in the original ORECA models, simplifications were introduced (and tested) in the MORECA modeling of radiation heat transfer between the upper and lower core surfaces and the vessel thermal shields. Rather than calculating radiation heat transfer between each of the 205 fuel element and reflector upper surfaces and the 205 surfaces of the vessel thermal shields, a concentric-ring approximation was used. Each ring represents a single ring of elements, with a ring of corresponding projected area of the thermal shield directly opposite. Hence, 7 rings are used to represent each surface. Equations for ring-to-ring heat transfer were derived from view factor equations for opposing disks given in Ref. A.6.

The view factor  $F_{12}$  for opposing disks 1 and 2, with radii  $r_1$  and  $r_2$ , separated by length  $L$  is:

$$F_{12} = \frac{1}{2} \left( x - \sqrt{x^2 - 4(R_2/R_1)^2} \right) \quad (\text{A.19})$$

where

$$\begin{aligned} x &= 1 + (1 + R_2^2)/R_1^2, \\ R_1 &= r_1/L \\ R_2 &= r_2/L \end{aligned}$$

The view factors for concentric disks to rings can be obtained by subtracting out the doughnut centers from disk-to-disk view factors. For example, to solve for the view factor for ring 2 to disk 3,  $F_{23}$  (see Fig. A.3),

$$A_1 F_{13} + A_2 F_{23} = A_{1+2} F_{(1+2)3} \quad (\text{A.20})$$

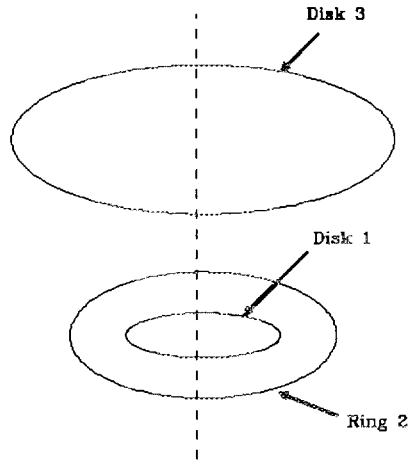


Fig. A.3. Ring-to-disk view factors.

$$F_{23} = \frac{A_{1+2}F_{(1+2)3} - A_1F_{13}}{A_2}, \quad (\text{A.21})$$

where  $A_1, A_3 =$  disk areas and  $A_2 =$  ring area.

Likewise, ring-to-ring view factors can be calculated by subtracting out the area-weighted view factor of a ring to an inner disk from the ring to the outer disk (see Fig. A.3).

Radiant heat transfer from the upper core surface to the side walls was also found to be significant. The view factor for each ring to the side walls is simply calculated by noting that the sum of the view factors for any ring should be 1.0, so the difference between 1.0 and the sum of its view factors to the opposing rings is its side wall view factor.

View factor calculations are done in subroutine VFRING and employed in subroutine TOPTTEM (upper plenum) and BOTTEM (lower plenum).

## A.6 CORE BARREL AND VESSEL TEMPERATURE MODELING

The nodalization scheme used for the core barrel and vessel accounts for azimuthal asymmetries by splitting the fuel and reflector sections into quadrants. Axial noding allocates one each to the upper and lower reflector areas and one for every two of the ten fuel element sections. Hence, in the fuel-reflector region, there are four quadrants times seven axial sections or 28 nodes each for the core barrel and vessel. In the upper and lower plenums, there are one each core barrel and vessel node for the side walls. The upper plenum ceiling and lower plenum floor are each represented by seven concentric ring nodes as described in the preceding section. The top of the vessel is represented by a single node. The bottom of the lower plenum floor is assumed to be well insulated, with heat transfer to the lower vessel head neglected.

Insulated thermal shields are utilized in various regions to protect the vessel from overtemperature; however, the placement of the shields and their thickness are design considerations which must account for the fact that the RCCS' heat removal effectiveness in a heatup accident requires high vessel temperatures. Insulation design must also consider that for pressurized heatup accidents the maximum temperatures occur near the top, while for depressurized scenarios they are near the vessel midplane.

In the current MORECA model, the insulation inside the vessel top head is assumed to consist of a thin thermal shield plate plus 1.25 in. of Kaowool. Insulation in the upper plenum side wall area and in the region adjacent to the upper reflectors is assumed to consist of a shield plate plus 0.75 in. of Kaowool. Radiation shield plates (without Kaowool) are assumed to be used in the lower plenum sidewall region.

The calculation of heat transfer through a radiation shield with conduction through insulation would normally involve iterations needed to determine the intermediate shield temperature. Instead, a straightforward explicit approximation was developed which gives good accuracy in the temperature ranges of interest. Equivalent heat transfer ( $h$ ) coefficients (for assumed emissivities of 0.8 for the core barrel, shield and vessel surfaces, along with unity view factors) are simple functions of the hot surface temperature  $T$  and the difference  $\Delta T$  between the hot and cold surfaces. Using the conductivity expression for Kaowool as

$$k = 0.1507 + T(1.349E-4 + 3.496E-8 T) , \quad (\text{A.22})$$

the approximate  $h$ 's for the two different insulation thicknesses are

$$h_{1.25 \text{ in.}} = 0.14 + 0.00231 T - 0.0014 \Delta T \quad (\text{A.23})$$

$$h_{0.75 \text{ in.}} = 0.00375 T - 0.0023 \Delta T, \quad (\text{A.24})$$

where

$$\begin{aligned} T &= \text{°F}, \\ k &= \text{Btu}/(\text{h}\cdot\text{ft}\cdot\text{°F}), \\ h &= \text{Btu}/(\text{h}\cdot\text{ft}^2\cdot\text{°F}). \end{aligned}$$

In the model of heat transfer between the core barrel and the vessel in the core region, the "view" between the two is  $\sim 50\%$  obscured by the rectangular inlet coolant ducts. Because a full radiation shield would cut the heat transfer rate by half, it is assumed that with 50% of the view obscured the heat transfer rate is reduced by 25%.

Core barrel to vessel heat transfer calculations are made in subroutines TOPTTEM for the upper plenum regions, BOTTEM for the lower plenum, and CONVEC for the middle vessel regions.

In response to a review critique, heat conduction between vessel nodes was added to the model. This was found to have negligible effects on computed vessel node temperatures ( $\sim 1^\circ\text{F}$  maximum) during core heatup accident scenarios. The calculations (which use temperature dependent steel conductivities) are done in subroutine VESCON.

## A.7 PRIMARY SYSTEM PRESSURE MODELING

Changes in primary system pressure are calculated by accounting for changes in primary system gas temperatures and inventories. The estimated pressure changes are strongly dependent on bulk gas temperatures in the steam generator and in relatively "dead" spaces, which together account for about 75% of the total mass of the primary system gas. Hence, the pressure calculated in core heatup transients is "approximate" and depends strongly on the details of steam generator cooldown operations. Those operations are crucial to the outcome of pressurized core heatup accidents because some (unlikely) scenarios could lead to pressures exceeding the relief valves' set point (1040 psi).

The primary system pressure calculation (as a function of temperature) is approximated in function PRESS by dividing the gas volume into four regions and solving the perfect gas law equation. For a given initial pressure  $P_0$  (925 psia) and volume absolute temperatures ( $T_{1-4}$  for volumes  $V_{1-4}$ ), the constant  $RMT$  for a fixed inventory is defined as:

$$RMT = P_0 \left( \frac{V_1}{T_1} + \frac{V_2}{T_2} + \frac{V_3}{T_3} + \frac{V_4}{T_4} \right) . \quad (A.25)$$

Subsequently, the primary pressure  $P$  is calculated from

$$P = \frac{RMT}{V_1/T_1 + V_2/T_2 + V_3/T_3 + V_4/T_4} . \quad (A.26)$$

Using the depressurization options, the pressure  $P$  can be ramped down to a new level at a specified rate, and when that target pressure is reached,  $RMT$  is recalculated. Thereafter, the new value of  $RMT$  corresponding to the reduced inventory is used to calculate  $P$ .

The four volumes are associated with the core coolant (560 ft<sup>3</sup>), core inlet plenum (8700 ft<sup>3</sup>), core outlet plenum (4350 ft<sup>3</sup>), and steam generator cavity (7390 ft<sup>3</sup>). For low primary system flows through the steam generator (<10%), it is assumed that the steam generator cavity gas temperature approaches the nominal feedwater temperature exponentially (arbitrarily assumed as a 30-min time constant); otherwise, it is computed as the average of the core inlet and outlet plenums.

## A.8 SHUTDOWN COOLING SYSTEM (SCS) MODELING

The SCS heat exchanger is a tube-in-shell design with pressurized water coolant in the tubes. For heat exchanger modeling, it is convenient to use dimensionless parameters and time constants for the heat transfer between each fluid and the tube (Ref. A.1). First, we define the "section length,"  $n$ , and the time constant based on heat transfer to the surface being heated or cooled,  $\tau$ :

$$n = \frac{hA}{WC_p} \quad (A.27)$$

and

$$\tau = \frac{MC_p}{hA} , \quad (\text{A.28})$$

where

$h$  = fluid-to-surface heat transfer coefficient, Btu/(h·ft<sup>2</sup>·°F);  
 $A$  = surface area of tube, ft<sup>2</sup>;  
 $WC_p$  = mass flow rate of the fluid, lb/h, times its specific heat, Btu/(lb·°F);  
 $\tau$  = time constant referenced to tube, h;  
 $MC_p$  = heat capacity of tube, Btu/°F.

Because the time response of the SCS is fast compared to that of the core in a shutdown cooling mode, it is reasonable to employ steady-state solutions and the concept of heat exchanger effectiveness. For example, the cooling effectiveness  $\epsilon_c$  is defined as

$$\epsilon_c = \frac{T_{Hi} - T_{Ho}}{T_{Hi} - T_{ci}} , \quad (\text{A.29})$$

where if hot helium outlet temperature  $T_{Ho}$  were equal to the cooling water inlet temperature,  $T_{ci}$ , the device would be 100% effective ( $\epsilon_c = 1.0$ ). For a counterflow heat exchanger,  $\epsilon_c$  can be calculated explicitly (Ref. A.7) by

$$\epsilon_c = \frac{1 - \exp[-(1 - N_1)N_2]}{1 - N_1 \exp[-(1 - N_1)N_2]} . \quad (\text{A.30})$$

In terms of the quantities defined previously,

$$N_1 = n_c \tau_c / n_H \tau_H \quad (\text{A.31})$$

$$N_2 = n_H / (1.0 + \tau_c / \tau_H) . \quad (\text{A.32})$$

A heat exchanger's heating effectiveness  $\epsilon_h$  can be calculated in a similar fashion. These equations are solved in subroutine CAHE, in that for given helium and water flows and inlet temperatures, the (steady-state) outlet temperatures can be computed directly. The SCS model in MORECA allows (user input) specification of the water and helium flows and the water inlet temperature. There is also a built-in automatic control function model (corresponding to the process design) which reduces the hot helium flow below the user-input value if the cooling water outlet temperature exceeds 400°F (to prevent boiling). This model is in the function routine FLOW.

## A.9 REACTOR CAVITY COOLING SYSTEM (RCCS) MODELING

For all reactor operating conditions, the reactor vessel (RV) will transfer heat by radiation and natural convection through the reactor cavity to the RCCS panels (Fig. A.4),

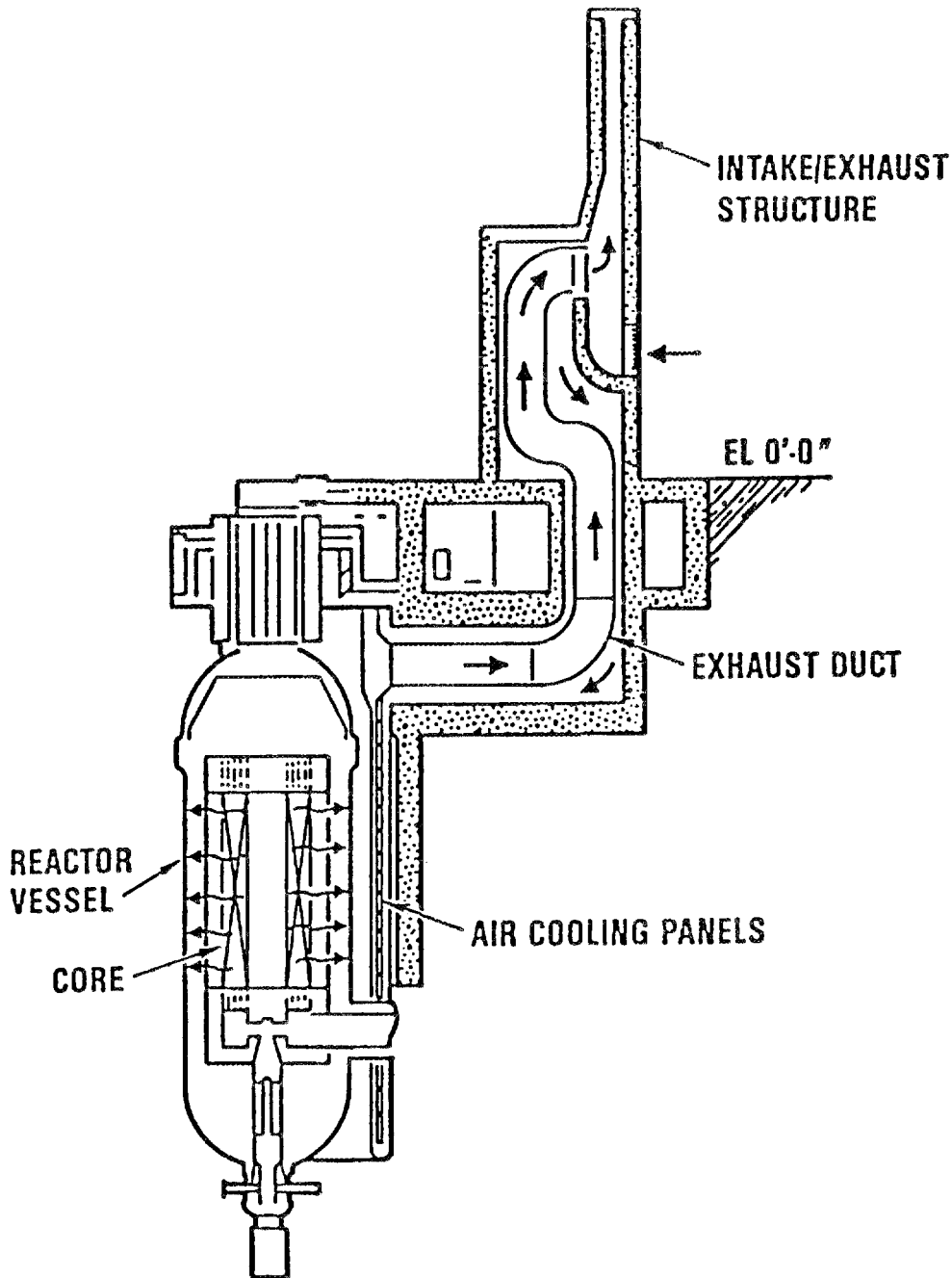


Fig. A.4. Passive reactor cavity cooling system. Source: U.S. Department of Energy, *Preliminary Safety Information Document for the Standard MHTGR*, HTGR-86-024, Vols. 1-5, 1986, plus ten amendments through February 1989 (this document is classified as "Applied Technology" and is not in the public domain; requests for this document should be made through the U.S. Department of Energy, Washington, D.C.).

where the heated air flow inside these panels is induced by buoyant forces (the chimney effect). The RCCS has no moving parts.

There are four quadrants of RCCS panels, each with an active heat transfer length of approximately 17 m. There also are four inlet/outlet structures with coaxial ducts, where the inner duct carries the hotter air from the reactor cavity and the outer duct carries the cooler ambient air. The height of interconnecting ducts is approximately 33 m above the panels. Redundancy is provided by interconnecting ducts and plenums to ensure that a natural convection flow of ambient air is available at all times.

The dynamic simulation of the RCCS is described in detail in a companion report (Ref. A.8). The model is implemented in a subroutine RCCS. The equations governing the air flow and the air heat transfer in the RCCS are coupled. Further coupling via radiation and convection occurs by the transfer of heat from the outer surface of the RV to the outer surface of the RCCS panels. For dynamic modeling of the heat transfer process, the simplifying assumption is made that there is negligible thermal and mass inertia on the air side relative to the thermal inertia of the metal panels. The use of this "quasi-static" assumption greatly simplifies the analysis and can be rigorously justified (Ref. A.9). The same assumption is made for the primary coolant in the core.

The conservation of energy equation for each of the nine RCCS panel nodes is a simple heat balance of the heat transferred by radiation and natural convection from the vessel and the heat convected to the air flowing upward in the channel. The flow of air through the RCCS ductwork, including the hot riser section of the panels, is modeled with the one-dimensional momentum equation adapted from Ref. A.2 for the core cooling channels. The outlet air temperature from each node is computed by using the exponential approach model, which is an exact solution of the differential equation for conservation of energy where the panel temperature is uniform over the node length, the air transit time is negligible, and the air thermophysical properties are constant. Thermal radiation heat transfer from the front face to the sides or back of the internal hot riser channel is neglected. The convective heat transfer from the side walls to the flowing air is modeled as an extended surface (Ref. A.10). The back face of the panel duct is treated as an adiabatic surface. The computed heat transfer to ambient conditions was found to be relatively insensitive to the value of the heat transfer coefficient on the air side of the RCCS panels.

The heat transfer process inside the reactor cavity from the uninsulated outer wall of the RV to the RCCS hot riser panels consists of natural convection and thermal radiation. Participating media thermal radiation heat transfer in the annular space between the RV and the RCCS panels is neglected in the analyses presented here but is being considered for postulated accidents in which steam or aerosols are present.

The net heat transferred by radiation from the RV to the RCCS panels is modeled with the assumption that all surfaces are gray and diffuse (i.e., the emissivities are independent of wavelength). Natural convection of heat across the cavity is also modeled but is much less than the radiant heat transfer across the annulus.

For natural-convection flow analysis, the conservation of energy and momentum equations for the fluid are coupled so that simultaneous solution is usually required. However, because the dynamics of the RCCS panel are much slower than the dynamics of the air, values of the air temperatures and flows will not appreciably change over a reasonably short time step. Therefore, panel temperatures from a previous time step are used in the equation to compute air flow.

## A.10 SPECIAL SOLUTION TECHNIQUES

To avoid the consumption-intensive task of solving all of the core heat conduction equations as a set of 2870 coupled differential equations, a "component isolation" technique was implemented. The basis of this method is the assumption of a model in which the component (i.e., the fuel element block) sees neighboring blocks with fixed temperatures over the time period  $\Delta t$ , the computation time interval. For example, consider the coupled equations for node temperatures  $T_i$ , where in hex geometry each node is coupled to six radial neighbors:

$$\begin{aligned}\frac{dT_1}{dt} &= -6\alpha T_1 + \alpha(T_2 + T_3 + T_4 + T_5 + T_6 + T_7) + \frac{Q_1}{MC_p} , \\ \frac{dT_2}{dt} &= -6\alpha T_2 + \alpha(T_1 + T_3 + T_4 + \dots) + \frac{Q_2}{MC_p} ,\end{aligned}\quad (\text{A.33})$$

etc., where

$$\alpha = \frac{D_H}{(\Delta X)^2}, \text{ min}^{-1} \quad (D_H = \text{heat diffusivity, } \Delta X = \text{spacing interval}) ,$$

$Q_i$  = heat generation rate in node  $i$ , Btu/min;  
 $MC_p$  = heat capacity of node, Btu/°F.

Expressed in matrix form,

$$\frac{dT}{dt} = AT + Z . \quad (\text{A.34})$$

The exact form of a recursive solution to Eq. (A.20), assuming  $Z_i$  stays constant over the time interval  $\Delta t$  is (Ref. A.11)

$$T(t + \Delta t) = e^{A\Delta t}T(t) + (e^{A\Delta t} - I)A^{-1}Z_i . \quad (\text{A.35})$$

The isolation technique incorporates the coupling to the adjacent nodes as part of the forcing function  $Z_i$ :

$$T_1(t + \Delta t) = e^{-6\alpha\Delta t}T_1(t) + \frac{e^{-6\alpha\Delta t} - 1}{-6\alpha} \left[ \alpha(T_2 + \dots + T_7) + \frac{Q_1}{MC_p} \right] . \quad (\text{A.36})$$

This method is similar to an Euler explicit solution; the major difference is that the first-order equations are solved exactly.

Another approximation used in MORECA is the sequential, rather than simultaneous, solution of the conduction and convection cooling equations. The dependence of the flow equations on temperature is derived from temperatures calculated at the previous time step. This approximation is verified by reducing the time interval  $\Delta t$  until there are no further significant changes in the results.

The individual fuel element column flow rates are computed at each time step by an iterative scheme that was developed by trial and error. The criteria to be satisfied are the percentage error of the calculated total flow  $\sum W_i$  compared with the specified total flow must be less than PERR or the absolute error must be less than AERR (where PERR and AERR are input via a DATA statement). Convergence is usually achieved within two or three iterations for reference values of PERR and AERR (1% and 1.0 lb/s respectively). The iteration scheme is as follows.

1. For the first try, if the total flow specified ( $WT$ ) is equal to the value of  $WT$  at the last time step, set the overall core  $\Delta P$  ( $DP$ ) equal to the last value of  $DP$ ; if not, compute

$$DP = (SDPW \cdot WT)^2 - BT \quad , \quad (41)$$

where

$$SDPW = [\sqrt{(DP+BT)}/WT]_{t=0} \quad , \quad (A.38)$$

$BT$ =summation of all static head terms in Eq. (A.16),

$$BT = \frac{LP}{R} \sum_{ij} \frac{1}{T_{ij}} \quad . \quad (A.39)$$

2. For the second try, compute

$$DP = \left( \frac{WT}{\sum_i W_i} \right)^2 (DPL + BT) - BT \quad , \quad (A.40)$$

where  $DPL$  is the last try value of  $DP$ .

This prediction tends to overreact for fast flow transients; so to compensate for this, a lower limit value of 0.1 is used for  $(WT/\sum W_i)$ . Also, if  $(WT/\sum W_i) < 0$ , then

$$DP = DPL + 0.7 [SDPW(WT - \sum_i W_i)]^2 \quad . \quad (A.41)$$

3. For the third try and thereafter, a linear interpolation scheme is used:

$$DP = DP1 + \left( \frac{WT - WA1}{WA2 - WA1} \right) (DP2 - DP1) \quad , \quad (A.42)$$

where  $DP1, 2$  = two previous try values of  $DP$ ; and  $WA1, 2$  = two previous try values of  $\sum W_i$ .

The program stops if convergence is not attained in MAXIT tries; MAXIT is specified in a DATA statement (= 20).

## A.11 FUEL FAILURE MODELS

Currently, MORECA has two different fuel failure models. The first is a simple temperature-only failure-dependence model that calculates the fraction of the total fuel that has, at any time, exceeded a user-specified "failure temperature." A second, more detailed model is based on work by D. T. Goodin of GA (Ref. A.12). This model predicts cumulative fuel failure fractions (*CFF*) that are dependent on the time the fuel spends at a given temperature. The failure rate is assumed to be a function of two process: a nonlinear mechanism due to decomposition and diffusion and a linear mechanism due to corrosion and diffusion. Because of the nonlinear dependence of the *CFF* on time at a certain temperature, the original Goodin equations had to be approximated by a linear model to accommodate arbitrary fuel temperature histories. Although this model includes the effects of time at temperature, it assumes that failures are independent of fuel age or burnup. Burnup effects are included in later models, which are not as yet implemented in MORECA.

The MORECA implementation of the Goodin model is in subroutine GOODVT. Characterization of the nonlinear decomposition term (the *B* component of Goodin's equation) by the sum of two (linear) exponentials improved the versatility of the model and allowed for decreasing temperatures. In the original model, "self healing" would occur (i.e., the fraction of failed fuel would decrease) if the fuel temperature decreased. The coefficients in the exponential approximation were determined by a gradient search routine, which found what appeared to be a global optimum set of coefficients. The resulting expression is

$$\text{Component } B = FB \left[ C_1 (1 - e^{-C_2 x}) + (1 - C_1) (1 - e^{-C_3 x}) \right] , \quad (\text{A.43})$$

where

*FB* = Goodin's  $f_B$  term for the nonlinear failure mechanism;

$x = \alpha t$ ;

$\alpha$  = Goodin's  $\alpha$  term;

$t$  = incremental time, h;

$C_1, C_2, C_3$  = coefficients in exponential approximation (= 0.237, 32.8, 1.35).

The rest of the fuel failure fraction calculation (made for each fuel element node) is taken directly from the Goodin reference.

From sensitivity studies, it was found that fuel failure calculations could use large computation time steps (many hours) with little degradation in accuracy, as long as the average of the temperature-dependent functions is representative of the true average (i.e., average values of failure rates are computed by using initial and final values of the individual component functions as opposed to using the function values computed at the average temperature over the interval).

## A.12 REFERENCES FOR APPENDIX A

- A.1. S. J. Ball, "Approximate Models for Distributed Parameter Heat Transfer Systems," *Trans. Instrum. Soc. Amer.*, 3(1), 38-47 (January 1964).

- A.2. S. J. Ball, *ORECA-I: A Digital Computer Code for Simulating the Dynamics of HTGR Cores for Emergency Cooling Analyses*, ORNL/TM-5159, Oak Ridge National Laboratory, Oak Ridge, Tenn., 1976.
- A.3. J. C. Cleveland, *CORTAP: A Coupled Neutron Kinetics-Heat Transfer Digital Computer Program for the Dynamic Simulation of the HTGR Core*, ORNL/NUREG/TM-38, Oak Ridge National Laboratory, Oak Ridge, Tenn., 1977.
- A.4. W. H. McAdams, *Heat Transmission*, 3d Ed., McGraw, New York, 1954.
- A.5. J. F. Petersen, *RECA3: A Computer Code for Thermal Analysis of HTGR Emergency Cooling Transients*, GA-A-14520, General Atomics, San Diego, 1977.
- A.6. A. J. Chapman, *Heat Transfer*, 2d Ed., p. 611, Macmillan, New York, 1967.
- A.7. W. H. Giedt, Chap. 13 in *Principles of Engineering Heat Transfer*, Van Nostrand, Princeton, N.J., 1961.
- A.8. J. C. Conklin, *Modeling and Performance of the MHTGR Reactor Cavity Cooling System*, ORNL/TM-11451, Oak Ridge National Laboratory, Oak Ridge, Tenn., 1990.
- A.9. J. C. Conklin, *Scaling Analysis of the Coupled Heat Transfer Process in the HTGR Core*, ORNL/TM-10099, Oak Ridge National Laboratory, Oak Ridge, Tenn., 1986.
- A.10. B. Gebhart, Chaps. 5 and 11 in *Heat Transfer*, 2d Ed., Macmillan, New York, 1967.
- A.11. S. J. Ball and R. K. Adams, *MATEXP, A General Purpose Digital Computer Program for Solving Ordinary Differential Equations by the Matrix Exponential Method*, ORNL/TM-1933, Oak Ridge National Laboratory, Oak Ridge, Tenn., 1967.
- A.12. D. T. Goodin, *Fuel Failure Model for MHTGR*, HTGR-85-107, Rev. 1, U.S. Department of Energy, 1985.



**Appendix B**

**MORECA INPUT VARIABLES**



## B.1 SUMMARY OF MORECA INPUT DECK OF SEQUENTIAL DATA FOR MHTGR COMMERCIAL DESIGN BATCH-INPUT SERIAL VERSION\*

<u>ROUTINE</u>	<u>CARD</u>	<u>VARIABLES</u>
MAIN	1	AL, QZ, DT, TM, DP, NTP, JSEQ, JPF, FSQ
	2	QRID, QR (20-85)
	3	PIN
INIT	4	TIP, TSGO, FTOTO, QBY, FHBP, FCBP, FBPLP
	5-209	XP (1-205, 1-14)
	210-213	TTOPV, TUVSW, VES (1-4, 1-7), TLVSW
CFLOW	214-222	CTOR (20-85)
End of input deck for 1st run.		
MAIN	223	AL, QZ, DT, TM, DP, NTP, JSEQ, JPF, FSQ (SET AL = 0.0 TO QUIT)

## B.2 ANNOTATED DESCRIPTIONS OF INPUT VARIABLES

AL =  $\alpha$  (Eq. A.19 in Appendix A) equivalent for hexagonal geometry.

See Eq. A.4 in Appendix A for terminology:

$$\alpha = \frac{k'A}{MC_p \Delta X} = 0.003097 (\text{min}^{-1}) \quad ,$$

where  $k'$  = effective reference conductivity corrected for hexagonal geometry  
 = 10 Btu/(h·ft·°F) × (4/6) × (1 h/60 min) (see Eq. A.3 in Appendix A)

M = mass =  $\rho V$  for hex block, lb, = 282.9 lb at reference density ( $\rho = 90 \text{ lb/ft}^3$ );

$\Delta X$  = characteristic length = 1.181 ft (hex center-to-center);

A = mean area =  $\Delta X \cdot L = 3.073 \text{ ft}^2$ ;

L = block length = 2.602 ft;

\*See alphabetized list of input variables with descriptions, Appendix C. The diskette submitted to the National Energy Software Center (NES-C) contains the MAIN program and 25 subprograms (in Fortran-77), a sample input deck and output file, plus the database programs and files (Appendix C).

$C_p$  = reference specific heat = 0.33 Btu/(lb°F);

$QZ = Q/MC_p$  (°F/min) reference  
 = average adiabatic core heatup rate for 99% of the 350 MW in the annular core with 660 fuel elements

$$= \frac{350 \text{ MW} * 56883 \text{ (Btu/min)/MW} * 0.99}{282.9 \text{ lb} * 660 \text{ (elements)} * 0.33 \text{ [Btu/(lb} \cdot \text{°F)]}} = 319.9 \text{ °F/min};$$

$DT$  = computation time step, min;

Notes:  $DT$ s of up to 10 min give good accuracy for depressurized LOFC heatup accidents; likewise up to 5 min for pressurized LOFCs. For substantial SCS flows, 1–2 min  $DT$ s may be needed. For full power/flow (steady state), 0.5-min  $DT$ s are needed.

$TM$  = maximum (stop) time for computation, min;

$DP$  = initial guess of core  $\Delta P$  at initial flow conditions, psi;

$NTP$  : printouts occur every  $NTP$  computation time steps;

$JSEQ$  = program control flag:

- = 0 : calculate transient using input initial conditions specified,
- = 1 : calculate initial conditions and write file for use in subsequent runs,
- = 2 : calculate transient using initial conditions from run 1;

$JPF$  = flow and  $\Delta P$  detail print flag:

- 1 : never,
- 0 : only at time = 0,
- 1 : print with each output;

$FSQ$  = core flow distribution flag [see detailed discussion in report (Sect. 3.2, Core Bypass Flow)]:

- 3 = using input values of core outlet temperatures [ $CTOR$  (20–85)], calculate heat balance value of cold bypass flow,
- 5 = use  $CTOR$  values for initial estimates, calculate flows using element (fixed) orifice coefficient;

*QRID* = comment line;

*QR* (20–85) = radial peaking factors, core element numbers 20–85;

*PI* = initial core inlet pressure, psia;

*TIP* = initial inlet temperature to vessel, °F;

*TSGO* = initial steam generator outlet temperature, °F;

*FTOT0* = initial total helium flow, lb/min;

*QBY* = fraction of total core power not generated in the fuel elements

*FHBP* = fraction of total primary helium flow bypassing the fuel elements and cooling the reflector elements (hot bypass);

*FCBP* = fraction of primary helium flow bypassing the fuel elements which is not heated (cold bypass);

*FBPLP* = fraction of cold bypass flow going directly from the vessel inlet to the lower plenum.

The following initial temperatures are calculated by using the *JSEQ* = 1 option:

*XP* (1–205, 1–14) = core (fuel/target and reflector) element initial temperatures, °F;

*TTOPV* = initial top vessel temperature, °F;

*TUVSW* = initial top sidewall vessel temperature. °F;

*VES* (1–4, 1–7) = initial vessel middle temperatures (in quadrants), °F;

*TLVSW* = initial bottom sidewall vessel temperature, °F;

*CTOR* (20–85) = fuel elements initial outlet temperatures, °F.



**Appendix C**

**MORECA PROGRAM DESCRIPTION DATABASES**



## C.1. PROGRAM DESCRIPTION DATABASES

Databases (using dBase-3+ or dBase-4) have been developed to assist MORECA code users with program interpretation, verification, and modification. The major database file consists of a listing of each program variable plus other essential information including a brief description, dimensions, what common block (if any) it appears in, where it is defined, and where (else) it is later modified. A flag in the description field, @, is used to denote variables that are read in as part of the input file. The virtue in putting all this information in a (large) relational database is that cross checking and special listings or searches can easily be done by simple dBase commands or programs. Examples are given in Sect. C.2. This major database file containing all of the program variables is called OREVAR, and it is optionally indexed alphabetically with the index file OVAR.

A second database file (ORECOM) lists all of the common blocks, what variables are in them, and what programs they appear in. This (small) file contains some redundant information (with OREVAR) but is useful for cross-checking to ensure that the user/checker/modifier is aware of the distribution of common variables.

The third database file (PROCAL) lists each program with information about what programs are called by it, what common blocks are in it, and what variables are in its argument list. Each record also has an accompanying Memo file that has a description of the function of each routine. This file also contains some redundant information but, again, is useful for cross-checking.

Although this collection of databases is "isolated" from the actual program, at least in terms of strict accountability, the use of selected database information in conjunction with a cross-reference (XREF) listing of a program facilitates verification of the proper placement, use, and spelling of each variable.

Currently, the variables in two of the programs are not included in the OREVAR database: (1) CAHE, which models the Shutdown Cooling System (SCS); and (2) RCCS (and its adjuncts RCCSD, RK4, CP, PRR, RHO, THERMK, and VISC), which models the air-cooled Reactor Cavity Cooling System (RCCS). The rationale for this omission is that these programs were written "independently" of MORECA and thus contain different program structural characteristics and variable naming conventions. They are also relatively "detached," so their absence is not crucial to checking the overall MORECA code. Detailed documentation of the RCCS code(s) is given by J. C. Conklin (Ref. C.1).

## C.2 EXAMPLE USES OF THE DATABASES

A simple dBase program OREP (Fig. C.1) can be used to get selective listings of the variables in OREVAR. For example, one can list all of the input variables (and their descriptors) by requesting printout of variables with symbol "@" contained in the DESCRIPTION field (Fig. C.2), which shows the features of the descriptors. The variable QR, for example (radial peaking factors, dimensioned 85), is passed between programs via an argument list (Arg), is defined (DEF), or in this case read in, in the MAIN program, and may be modified in subroutine CFLOW.

As another example, OREP can also list all the variables in the OREVAR database that are in a given common block by requesting the field "com" to be searched for (for example) "PASS" (Fig. C.3). Note that search strings are case sensitive.

The example shown in Fig. C.4 can be used to cross-check the summary listing in the ORECOM file. Note that all the variables in the ORECOM file for the PASS

```

orep.prg 03/20/91

* OREP.PRG - Program to mess with OREVAR files
USE orevar INDEX ovar
_pquality=.T.
ACCEPT " Field name to be searched (var des dim com def mod) = " TO fn
* To get a complete listing, enter "!" for phrase
ACCEPT " Phrase to search for = " TO phr
?
?" VAR          DESCRIPTION          DIMENS  COM    DEF    MOD"
?
GO TOP
lctr=0
* first page line limit = 55
lctrlim=55
DO WHILE .NOT. EOF()
IF phr $ &fn .OR. phr = "!"
? var, des, dim, com, def, mod
lctr=lctr+1
IF lctr = lctrlim
lctr=0
* line limit after first page = 58
lctrlim=58
* skip 8 lines for total lines/page = 66
?
?
?
?
?
?
?
?
ENDIF
ENDIF
SKIP
ENDDO
CLOSE DATABASES

```

Fig. C.1. OREP program.

```

. do orep
  Field name to be searched (var des dim com def mod) = des
  Phrase to search for = @

  VAR          DESCRIPTION          DIMENS  COM   DEF   MOD
AL             @Alpha - reference diffusivity 1             MAIN
CTOR          @Core outlet temps - initial  90             CFLOW
DP            @Core pressure drop          1             Arg    MAIN  CFLOW
DT            @Computation time step (min.) 1             LCSR   MAIN
FBPLP        @Cold bypass to lower plenum  1             PASS   INIT  CFLOW
FCBP         @Unheated bypass fraction     1             PASS   INIT  CFLOW
FHBP         @Heated bypass fract         1             PASS   INIT  CFLOW
FSQ          @Channel flow distrib flag   1             Arg    MAIN
FTOTO        @Initial value of total flow  1             Arg    INIT
JPF          @Print control flag          1             Arg    MAIN
JSEQ        @Run control flag             1             Arg    MAIN
NTP          @No of time steps between prnt 1             MAIN
PIN          @Core inlet pressure         1             Arg    MAIN
QBY         @Fract. Q=hot bypass          1             PASS   INIT
QR          @Radial peaking factors       85            Arg    MAIN  CFLOW
QRID        @Label for radial peaking fact 20             MAIN
QZ          @Full power F/min             1             PASS   MAIN  CFLOW
TIP         @Inlet plenum temperature     1             LCSR   INIT  MAIN
TM          @Max time for computation(min) 1             MAIN
TSGO        @Steam gen outlet temp (avg)  1             Arg    INIT  MAIN, CFLOW
XP          @Fuel/reflectr node temp-saved 206,14      Arg    INIT  MAIN

```

Fig. C.2. MORECA input variables.

```

. do orep
  Field name to be searched (var des dim com def mod) = com
  Phrase to search for = PASS

  VAR          DESCRIPTION          DIMENS  COM   DEF   MOD
CBFLP        Split cold bypass - fract-LP  1             PASS   CFLOW
FBPLP        @Cold bypass to lower plenum  1             PASS   INIT  CFLOW
FBYP         Core bypass flow fraction     1             PASS   INIT  CFLOW
FCBP         @Unheated bypass fraction     1             PASS   INIT  CFLOW
FHBP         @Heated bypass fract         1             PASS   INIT  CFLOW
QBY         @Fract. Q=hot bypass          1             PASS   INIT
QC          Node convection etc heat out  205,14      PASS   CONVEC TOPTEM,BOTTEM
QZ          @Full power F/min             1             PASS   MAIN  CFLOW
T           Time, min                     1             PASS   MAIN

```

Fig. C.3. Listing of variables in common block PASS.

```

. use orecom
. list
Record#  COMM  CVARs
PROGS
  1  PASS   T QC QZ QBY FHBP FCBP FBYP FBPLP CBFLP
MAIN CFLOW CONVEC POW INIT RCCS TOPTM BOTTEM OUTNOS FLOW TIN PRESS
  2  ORIFIC ORIOPN DPCOM
MAIN CFLOW CONVEC OUTNOS
  3  CAHEV  COMF COMT TOPC COMCO TMMAX HG2 JCAHE
MAIN FLOW TIN PRESS OUTNOS
  4  LCSR   DT PINC TIP TOP
MAIN CONVEC POW INIT OUTNOS RCCS TOPTM BOTTEM CAHE PRESS
  5  GBYE   FVT NGFAIL JGOOD GOODFF
MAIN OUTNOS
  6  LCS    QLUPG TCP TGP QLLPG TUPSW TLPSW QLUP TLUPT QLUPT QLLPS QLLPB
CONVEC OUTNOS TOPTM BOTTEM
  7  VESRC  QVLRC QVRC QVURC QVTRC TPANEL HEAT TOUTF AFOUTE
CONVEC OUTNOS RCCS TOPTM BOTTEM
  8  CBVES  CB VES TTOPV TUVSW TLVSW
OUTNOS CONVEC RCCS BOTTEM TOPTM

```

**Fig. C.4. ORECOM file of variables in common blocks and subroutines in which they appear.**

common block are indeed listed in the OREP search (and there is a 1-to-1 correspondence).

Note also that one can get a partial cross-check on the program listings. In the OREP search, the programs CFLOW, INIT, CONVEC, TOPTM, BOTTEM, and MAIN are all listed at least once, indicating that one or more variables in PASS were defined or modified in each of these programs. If one of these programs did not appear in the ORECOM list, it would imply an error of omission. The fact that there is not a 1-to-1 correspondence is not necessarily a problem, however, because some programs use the variables without modifying them.

To do a thorough checkout of the correspondence between the OREVAR variable listing and a program's coding (via a cross-reference or XREF output option in the Fortran compilation), OREP can be asked to look for that program name in both the DEFine field and the MODify field. There should be a one-to-one correspondence between the OREP listings and the XREF variable lists showing those that are calculated (=) and/or defined by DATA statements (D). An example of this application for the subroutine BOTTEM is shown in Fig. C.5.

A complete listing for all the variables (var) is obtained by using "!" as the search character in the OREP program.

. do orep

Field name to be searched (var des dim com def mod) = def  
 Phrase to search for = BOTTEM

VAR	DESCRIPTION	DIMENS	COM	DEF	MOD
ASWL	Area - vessel lower sidewall	1		BOTTEM	
QLLPB	Q from lower cp's to vessel =0	1	LCS	BOTTEM	
QLLPB	Q loss from CBs to bottom ves	1	LCS	BOTTEM	
QLLPG	Q loss from lower plenum gas	1		BOTTEM	
QLLPS	Q loss, l.p. liner to vessel	1	LCS	BOTTEM	
RVFL	Ring view factors for low refl	7	Arg	BOTTEM	
SWMCPA	Side wall heat capacity/ft2	1		BOTTEM	
TLPSW4	Lower plenum SW temp **4	1		BOTTEM	
TLPSW4	4th power of TLPSW	1		BOTTEM	

. do orep

Field name to be searched (var des dim com def mod) = mod  
 Phrase to search for = BOTTEM

VAR	DESCRIPTION	DIMENS	COM	DEF	MOD
AR	Top area of refueling region	1		TOPTTEM & BOTTEM	
AREA	Intermediate area AR, ASR ft2	1		TOPTTEM & BOTTEM	
ARING	Reflector ring areas ft2	7		TOPTTEM & BOTTEM	
ASR	Top area of side reflector ft2	1		TOPTTEM & BOTTEM, CONVEC	
BOLE8	Boltzmann constant * E8	1		CONVEC & TOPTTEM, BOTTEM	
CPMCPA	"coverplate" heat capacity/ft2	1		TOPTTEM & BOTTEM	
CPSWMC	Sidewall coverplate heat capac	1		TOPTTEM & BOTTEM	
EEBOL	Emissivity-Boltzmann factor	1		TOPTTEM & BOTTEM	
EL	Emissivity of lower surface	1		TOPTTEM & BOTTEM	
ES	Emissivity of sidewall surface	1		TOPTTEM & BOTTEM, CONVEC	
EU	Emissivity of upper surface	1		TOPTTEM & BOTTEM	
HT	Plenum height, ft	1		TOPTTEM & BOTTEM	
ICALL	First call flag (=0 on first)	1		TOPTTEM & BOTTEM, CONVEC	
JB	Beginning of ring index	1		TOPTTEM & BOTTEM, CONVEC	
JE	End of ring index	1		TOPTTEM & BOTTEM, CONVEC	
JRB	Beginning index-ring viewfacts	7		TOPTTEM & BOTTEM	
JRE	End index, ring viewfactors	7		TOPTTEM & BOTTEM	
NRRING	Ring counter	7		TOPTTEM & BOTTEM	
QC	Node convection etc heat out	205,14	PASS	CONVEC TOPTTEM, BOTTEM	
QGC	Intermediate heat transfer	1		TOPTTEM & BOTTEM	
QGCP	Heat gain by coverplates	7		TOPTTEM & BOTTEM	
QHT4	T**4 heat transfer intermed	7,7		TOPTTEM & BOTTEM	
QLTR	Top reflector heat transfer	205		TOPTTEM & BOTTEM	
QLTRR	Top reflector ring heat xfr	7		TOPTTEM & BOTTEM	
QSW	Intermediate heat transfer	1		TOPTTEM & BOTTEM	
QSWCP	Q to Plenum sidewall liner	1		TOPTTEM & BOTTEM	
QSWPR	Q to sidewall per ring	1		TOPTTEM & BOTTEM	
RRMCP	Region heat capacity	1		CONVEC + TOPTTEM, BOTTEM	
SWRF	Radiant heat transfer factor	1		CONVEC & TOPTTEM, BOTTEM	
T4A	Intermediate var - Avg temp	1		TOPTTEM & BOTTEM	
TC4	4th power factor for TCP & G	7		TOPTTEM & BOTTEM	
TGP	Lower plenum "cover plate" Ts	7	LCS	CONVEC BOTTEM	
TLPSW	Lower plenum sidewall temp	1	LCS	CONVEC BOTTEM	
TLVSW	Lower vessel sidewall temp	1	CBVES	CONVEC BOTTEM	
TR4A	4th power reflector ring temp	7		TOPTTEM & BOTTEM	
VESMCA	Vessel heat capacity per area	1		TOPTTEM & BOTTEM	

Fig. C.5. Listing of variables defined and modified in subroutine BOTTEM.

Other programs and listings available are the PPCAL program and its product, a listing of the PROCAL file. Note that in the PROCAL file, the argument names shown are as they are given in that subroutine or function and are not necessarily the same as those in the calling program. In running PPCAL, the user has the option of getting a screen display or a printout and getting the program descriptions listed, or not, with the other information. Output from a printout run of the PPCAL program with the program descriptions is shown in Fig. C.6, and a listing of PPCAL in Fig. C.7. A third program, DIDMOD (Fig. C.8), can be used (with caution) to make global changes to the OREVAR database.

### C.3 REFERENCE FOR APPENDIX C

- C.1 J. C. Conklin, *Modeling and Performance of the MHTGR Reactor Cavity Cooling System*, ORNL/TM-11451, Oak Ridge National Laboratory, Oak Ridge, Tenn., 1990.

```
. do ppcal
Include summary descriptions of each routine (Y/N)? y
Output to printer (P) or screen (S)? p
```

PROCAL LISTING 03/20/91

```
Program - ALGEN
Calls =
Coms =
Args = NRR I J I1 I2 I3 I4 I5 I6 ALR ALRU ALRD SALR XKR XKA
```

Subroutine ALGEN generates the average of the diffusivity ratios for core nodes neighboring the selected (i,j) node.

```
-----
Program - AXIK
Calls =
Coms =
Args = T I J
```

Function AXIK computes core node axial conductance as a function of temperature and material. A flag (KCH) can be set to choose between the latest GA MHTGR correlations or the Fort St. Vrain FSAR correlations.

```
-----
Program - BOTTEM
Calls = VFRING
Coms = LCS LCSR CBVES VESRC PASS
Args = X
```

Subroutine BOTTEM is used to calculate heat transfer in the lower plenum region, including radiant heat transfer from the core support blocks to the floor and side walls using ring nodes (see VFRING). Node temperature averaging to obtain an effective ring temperature for radiant heat transfer is done on the basis of its 4th power. A simple model (with fixed h) is used for convection heat loss to the side wall coverplates. Heat transfer from the floor to the bottom vessel wall is neglected. Coverplate and vessel wall temperature updates are done via Euler approximations.

Fig. C.6. PROCAL listing.

Program - CAHE  
 Calls =  
 Coms = LCSR  
 Args = THI THO TCI TCO WH WC TMMAX HG2

Subroutine CAHE is used to calculate the performance of the shutdown cooling system (SCS). It makes use of the analytical steady-state solution for single-phase counterflow heat exchanger behavior given both hot and cold side inlet temperatures and flow. The variable helium and coolant water properties are accounted for. A single average tube model is used. CAHE takes advantage of the fact that the response time of the SCS heat exchanger is much shorter than that of the core it is cooling, especially during low-flow "shutdown" conditions.

-----

Program - CFLOW  
 Calls = CONVEC SUMW  
 Coms = PASS ORIFIC  
 Args = X CF FTOT QR PIN DP IC TO TREV JSEQ RE FSQ JPF

Subroutine CFLOW computes the flows in each of the fuel elements individually. The flow effective resistance for an element is computed using a weighted average accounting for the number and differences in the coolant hole sizes. Fuel element bypass flows are also computed based on input values of initial bypass flow fractions and thereafter assuming fixed orifice characteristics. Flow resistances are based on viscosity calculated at the mean channel temperature, and account for laminar, turbulent, and transition flow regions. Buoyancy forces allow for flow in some elements to be reversed (upward) while other are downward, with or without forced circulation. An iterative scheme is used to determine a net plenum-to-plenum pressure difference which satisfies the net total flow (input) requirement to within specified (input) error bounds.

-----

Program - CONVEC  
 Calls = BOTTEM RCCS TOPTM VESCON  
 Coms = PASS ORIFIC LCS LCSR CBVES VESRC  
 Args = X CF TO TREV RE STI SCFN FTOT TSGO TINP

Subroutine CONVEC computes the convection heat transfer in each of the fuel elements in the core, accounting for variations in both flow regime and direction. An average reflector (or heated bypass) flow is used. Average plenum temperatures are calculated assuming well-mixed flow-weighted averages of all contributing inputs. Approximate heat capacities of the core support posts are included in the lower plenum mixed-mean temperature calculation. Core barrel and coverplate to vessel nodes heat transfer is also calculated. The inlet plenum inlet temperature is dependent on a computed temperature rise across the circulator and heat transfer in the (upflow) channels adjacent to the core barrel. Calls to the subroutines for reactor cavity cooling system performance (RCCS), vessel conduction heat transfer (VESCON), and upper and lower plenum heat transfer (TOPTM and BOTTEM) are made from CONVEC.

Program - CP  
 Calls =  
 Coms =  
 Args = T

Function CP calculates air specific heat as a function of temperature for the RCCS model.

-----

Program - GOODVT  
 Calls =  
 Coms =  
 Args = TEMPF AP FBP SP FLO SLO DT FVT

Subroutine GOODVT implements the Goodin model for fuel failure as a function of time and temperature for each fuel element node.

-----

Program - INIT  
 Calls =  
 Coms = PASS LCSR  
 Args = XP TSGO FTOTO QA

Subroutine INIT is called in MAIN to input the bulk of the initial condition data. In recent revisions, it now reads in all of the core nodes and the vessel nodes.

-----

Program - MAIN  
 Calls = ALGEN AXIK CAHE CFLOW FLOW INIT OUTNOS POW PRESS RADK SUBS TIN  
           TPROP CONVEC  
 Coms = PASS ORIFIC CAHEV LCSR GBYE  
 Args =

MORECA's MAIN program controls most of the action between subroutines, and does some variable initialization, data inputting, and calculations. Some of the initialization is done by calls to other subroutines, including FLOW, TIN, CAHE, INIT, PRESS, CFLOW, and CONVEC. MAIN contains the main loop which controls the progression of the simulation thru the time steps. It also computes the 3-D core (solid) node temperatures. The temperature-dependent conductance between blocks is obtained from calls to functions RADK and AXIK, with effective conductance between individual blocks computed in subroutine ALGEN. For each element (node), the neighboring node identifiers are obtained from subroutine SUBS. Variable node physical properties are called from subroutine TPROP. Inlet temperature, flow, pressure, and afterheat information is obtained via calls to TIN, FLOW, PRESS, and POW, respectively. Detailed and/or summary outputs are generated via calls to subroutine OUTNOS.

-----

Fig. C.6 (continued)

Program - OUTNOS  
 Calls = GOODVT  
 Coms = PASS LCS LCSR CBVES VESRC CAHEV ORIFIC GBYE  
 Args = X ALPH QT FT CF TREV RE PIN TSGO

Subroutine OUTNOS provides the output for a variety of options at specified intervals, including some post-processing to obtain variables that are not needed at each computation time interval. The calls to subroutine GOODVT and the accounting needed for fuel failure calculations are also done in OUTNOS.

-----  
 Program - POW  
 Calls =  
 Coms = PASS LCSR  
 Args = I

Function POW calculates the afterheat, fraction of initial power, using either the MHTGR PSID correlation, the MHTGR "best estimate" (HTGR-86-109) or the Fort St. Vrain FSAR correlation.

-----  
 Program - PRESS  
 Calls =  
 Coms = CAHEV LCSR PASS  
 Args = FT TO P0 IC

Function PRESS provides a simplified primary system constant-inventory pressure calculation based on a detailed averaging of gas volume temperatures in the reactor vessel but only a cursory approximation in the steam generator. Programmed depressurization can be introduced, where the pressure is ramped downward at a specified rate. Full depressurization is assumed to occur if the relief valve limit is reached. If depressurization is to an intermediate pressure, it is computed subsequently based on constant inventory at the end point; otherwise, it stays at atmospheric. Approximations to the steam generator average gas volume temperature are computed in PRESS.

-----  
 Program - PRR  
 Calls = CP THERMK VISC  
 Coms =  
 Args = T

Function PRR computes air Prandtl number from calls to VISC, CP, and THERMK for the RCCS model.

-----

Fig. C.6 (continued)

Program - RADK  
 Calls =  
 Coms =  
 Args = T I J

Function RADK computes core node radial conductance as a function of temperature and material. A flag (KCH) can be set to choose between the latest GA MHTGR correlations or the Fort St. Vrain FSAR correlations.

-----  
 Program - RCCS  
 Calls = CP PRR RCCSD RHO RK4 THERMK VISC  
 Coms = CBVES VESRC LCSR PASS JCC  
 Args = TINF

Subroutine RCCS provides the heat loss terms to the passive, air-cooled reactor cavity cooling system (RCCS) from the corresponding vessel nodes in an array QLOSS. The RCCS model is divided up into 4 quadrants with 9 axial nodes per quadrant. Details are given in J. C. Conklin's report ORNL/TM-11451.

-----  
 Program - RCCSD  
 Calls = CP PRR RHO THERMK VISC  
 Coms = JCC  
 Args = T TP TPDOT

Subroutine RCCSD provides detailed calculations of RCCS heat transfer for its calling routine, RCCS.

-----  
 Program - RHO  
 Calls =  
 Coms =  
 Args = T

Function RHO computes air density as a function of temperature (assuming atmospheric pressure) for the RCCS model.

-----  
 Program - RK4  
 Calls = F?  
 Coms =  
 Args = F Y T DT

Subroutine RK4 provides a 4th order Runge-Kutta solution for the RCCS model.

-----

Fig. C.6 (continued)

Program - SUBS  
 Calls =  
 Coms =  
 Args = I NRR I1 I2 I3 I4 I5 I6

Subroutine SUBS provides the array indices (subscripts) for neighboring nodes of the reference (i,j) node.

-----

Program - SUMW  
 Calls =  
 Coms =  
 Args = A B RAC PS DP WTA

Subroutine SUMW is used to sum the individual fuel element flows as computed in CFLOW for each iteration in the solution for plenum-to-plenum pressure drop.

-----

Program - THERMK  
 Calls =  
 Coms =  
 Args = T

Function THERMK calculates air thermal conductivity as a function of temperature for the RCCS model.

-----

Program - TOPTM  
 Calls = VFRING  
 Coms = LCS LCSR PASS CBVES VESRC  
 Args = X

Subroutine TOPTM is used to calculate heat transfer in the upper plenum region, including radiant heat transfer from the core plenum element blocks to the top and sidewall coverplate ring nodes (see VFRING). Node temperature averaging to obtain an effective ring temperature for radiant heat transfer is done on the basis of its 4th power. A simple model (with fixed h) is used for convection heat loss to the upper and side wall coverplates. Coverplate and vessel wall temperature updates are done via Euler approximations.

-----

Fig. C.6 (continued)

Program - TPROP  
Calls =  
Coms =  
Args = T I J ALFT QFACT XKR

Subroutine TPROP calculates the temperature-dependent diffusivity for the core nodes, and accounts for the geometry and composition differences according to node position.

-----

Program - VESCON  
Calls =  
Coms = CBVES  
Args = QCONV

Subroutine VESCON computes the negligible conduction heat transfer between vessel nodes.

-----

Program - VISC  
Calls =  
Coms =  
Args = T

Function VISC calculates air viscosity as a function of temperature for the RCCS model.

-----

Fig. C.6 (continued)

```

ppcal.prg 03/20/91

*PPCAL.PRG - Program to print PROCAL listing in readable form
USE procal INDEX proc
GO TOP
CLEAR
SET MEMOWIDTH TO 65
_plineno=0
_pquality=.T.
spl5=SPACE(15)
WAIT "Include summary descriptions of each routine (Y/N)? " TO yn
WAIT "Output to printer (P) or screen (S)? " TO ps
IF UPPER(ps)="P"
    SET PRINT ON
ENDIF
?
?"                               PROCAL LISTING ",DATE()
?
?
DO WHILE .NOT. EOF()
? "Program - ", prog
? "Calls =", calls
IF calls2#spl5
? SPACE(8),calls2
ENDIF
? "Coms =", com
? "Args =", args
?
IF UPPER(yn)="Y"
? mem
ENDIF
IF UPPER(ps)="S"
    WAIT
    CLEAR
ELSE
?
?"-----"
?
    SET PRINT OFF
    WAIT " <Rtn> to continue printing " TO yx
    SET PRINT ON
ENDIF
SKIP
ENDDO
IF UPPER(ps)="P"
    SET PRINT OFF
ENDIF
CLOSE DATABASES

```

Fig. C.7. PPCAL program.

```
didmod.prg 03/20/91

* DIDMOD.PRG - program to diddle with MOD or other field entries
USE orevar INDEX ovar
ACCEPT "Field to diddle with = " TO fdid
ACCEPT "String to search for = " TO sfind
ACCEPT "String to replace it with = " TO srep
GO TOP
DO WHILE .NOT. EOF()
IF sfind $ &fdid
    REPLACE &fdid WITH srep
    ? var, &fdid
ENDIF
SKIP
ENDDO
```

**Fig. C.8. DIDMOD program.**



NUREG/CR-5712  
 ORNL/TM-11823  
 Dist. Categories R1, R7, R8

### INTERNAL DISTRIBUTION

- |      |                  |        |                                  |
|------|------------------|--------|----------------------------------|
| 1-5. | S. J. Ball       | 24-25. | C. E. Pugh                       |
| 6.   | W. P. Barthold   | 26.    | J. P. Sanders                    |
| 7.   | H. R. Brashear   | 27.    | O. L. Smith                      |
| 8.   | C. R. Brittain   | 28.    | O. M. Stansfield                 |
| 9.   | N. E. Clapp      | 29.    | J. D. White                      |
| 10.  | J. C. Cleveland  | 30.    | R. P. Wichner                    |
| 11.  | J. C. Conklin    | 31.    | T. L. Wilson                     |
| 12.  | B. G. Eads       | 32.    | R. E. Uhrig                      |
| 13.  | D. N. Fry        | 33.    | A. Zucker                        |
| 14.  | S. R. Greene     | 34.    | J. B. Ball, Advisor              |
| 15.  | F. J. Homan      | 35.    | P. F. McCrea, Advisor            |
| 16.  | J. E. Jones, Jr. | 36.    | T. B. Sheridan, Advisor          |
| 17.  | P. R. Kasten     | 37.    | ORNL Patent Section              |
| 18.  | H. D. Kerr       | 38.    | Central Research Library         |
| 19.  | T. S. Kress      | 39.    | Y-12 Technical Reference Section |
| 20.  | D. W. McDonald   | 40.    | Document Reference Section       |
| 21.  | D. R. Miller     | 41-42. | Laboratory Records Department    |
| 22.  | L. C. Oakes      | 43.    | Laboratory Records (RC)          |
| 23.  | D. L. Moses      | 44.    | I&C Division Publications Office |

### EXTERNAL DISTRIBUTION

45. Director, Division of Regulatory Applications, Office of Nuclear Regulatory Research, U.S. Nuclear Regulatory Commission, Washington, DC 20555
46. F. C. Chen, U.S. Department of Energy, NP-62, Washington, DC 20585
47. J. N. Donohew, Office of Nuclear Reactor Regulation, U.S. Nuclear Regulatory Commission, Washington, DC 20555
48. E. F. Goodwin, Office of Nuclear Reactor Regulation, U.S. Nuclear Regulatory Commission, Washington, DC 20555
49. W. B. Hardin, Division of Regulatory Applications, Office of Nuclear Regulatory Research, U.S. Nuclear Regulatory Commission, NL/S-169, Washington, DC 20555
50. J. M. Kendall, PDCO, MHTGR-NE, P.O.Box 85608, San Diego, CA 92138
51. Dr. Peter G. Kroeger, Brookhaven National Laboratory, Upton, NY 11973
52. C. Rodriguez, CEGA, MS 37-236, P.O. Box 85608, San Diego, CA 92138-5608
53. Dr. Zoltan Rosztoczy, Office of Nuclear Regulatory Research, U.S. Nuclear Regulatory Commission, Washington, DC 20555
54. Dr. Peter M. Williams, Director, Division of HTGRs, NE-451, U.S. Department of Energy, Washington, DC 20585
55. Office of Assistant Manager for Energy Research and Development, U.S. Department of Energy, Oak Ridge Operations, P.O. Box 2001, Oak Ridge, TN 37831-8600
- 56-67. Office of Scientific and Technical Information, U.S. Department of Energy, P.O. Box 62, Oak Ridge, TN 37831
- 68-292. Given distribution as shown in categories R1, R7, and R8



**BIBLIOGRAPHIC DATA SHEET**

*(See instructions on the reverse)*

1. REPORT NUMBER  
*(Assigned by NRC. Add Vol., Supp., Rev.,  
and Addendum Numbers, if any.)*

NUREG/CR-5712  
ORNL/TM-11823

2. TITLE AND SUBTITLE

MORECA: A Computer Code for Simulating Modular High-  
Temperature Gas-Cooled Reactor Core Heatup Accidents

3. DATE REPORT PUBLISHED

MONTH	YEAR
October	1991

4. FIN OR GRANT NUMBER  
A9477

5. AUTHOR(S)

S. J. Ball

6. TYPE OF REPORT

Technical

7. PERIOD COVERED *(Inclusive Dates)*

8. PERFORMING ORGANIZATION -- NAME AND ADDRESS *(If NRC, provide Division, Office or Region, U.S. Nuclear Regulatory Commission, and mailing address; if contractor, provide name and mailing address.)*

Oak Ridge National Laboratory  
Oak Ridge, TN 37831-6285

9. SPONSORING ORGANIZATION -- NAME AND ADDRESS *(If NRC, type "Same as above"; if contractor, provide NRC Division, Office or Region, U.S. Nuclear Regulatory Commission, and mailing address.)*

Division of Regulatory Applications  
Office of Nuclear Regulatory Research  
U.S. Nuclear Regulatory Commission  
Washington, DC 20555

10. SUPPLEMENTARY NOTES

11. ABSTRACT *(200 words or less)*

The design features of the modular high-temperature gas-cooled reactor (MHTGR) have the potential to make it essentially invulnerable to damage from postulated core heatup accidents. This report describes the ORNL MORECA code, which was developed for analyzing postulated long-term core heatup scenarios for which active cooling systems used to remove afterheat following the accidents are not necessarily available. Simulations of long-term loss-of-forced-convection (LOFC) accidents, both with and without depressurization of the primary coolant, have shown that maximum core temperatures stay below the point at which any significant fuel failures and fission product releases are expected. Sensitivity studies also have been done to determine the effects of errors in the predictions due both to uncertainties in the modeling and to the assumptions about operational parameters. MORECA models the U.S. Department of Energy (DOE) reference design of a standard MHTGR. This program was sponsored by the U.S. Nuclear Regulatory Commission (NRC) to assist in the preliminary determinations of licensability of the reactor design.

12. KEY WORDS/DESCRIPTORS *(List words or phrases that will assist researchers in locating the report.)*

modular HTGR  
safety analysis  
MORECA computer code  
dynamic simulation  
loss-of-forced-convection accidents  
depressurization accidents

13. AVAILABILITY STATEMENT

Unlimited

14. SECURITY CLASSIFICATION

*(This Page)*

Unclassified

*(This Report)*

Unclassified

15. NUMBER OF PAGES

16. PRICE